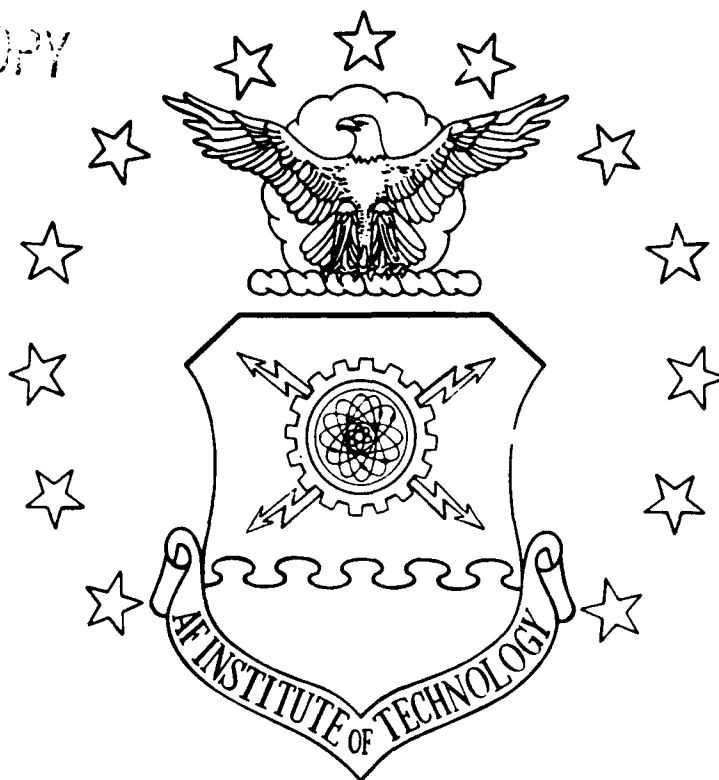


AD-A230 426

DTIC FILE COPY

1



DTIC

ELECTE

JAN 07 1991

D

THE USE OF THE LOWTRAN7  
ATMOSPHERIC TRANSMITTANCE AND RADIANCE  
COMPUTER PROGRAM FOR DETECTION  
SYSTEM DESIGN AND ANALYSIS

THESIS

Kelli J. Owen, Second Lieutenant, USAF

AFIT/GEP/ENP/90D-3

DISTRIBUTION STATEMENT A

Approved for public release  
Distribution Unlimited

DEPARTMENT OF THE AIR FORCE

AIR UNIVERSITY

**AIR FORCE INSTITUTE OF TECHNOLOGY**

Wright-Patterson Air Force Base, Ohio

91 1 3 110

1

DTIC  
ELECTE  
JAN 07 1991  
S D D

THE USE OF THE LOWTRAN7  
ATMOSPHERIC TRANSMITTANCE AND RADIANCE  
COMPUTER PROGRAM FOR DETECTION  
SYSTEM DESIGN AND ANALYSIS

THESIS

Kelli J. Owen, Second Lieutenant, USAF

AFIT/GEP/ENP/90D-3

THE USE OF THE LOWTRAN7 ATMOSPHERIC  
TRANSMITTANCE AND RADIANCE MODEL FOR DETECTION  
SYSTEM DESIGN AND ANALYSIS

THESIS

Presented to the Faculty of the School of Engineering  
of the Air Force Institute of Technology  
Air University  
In Partial Fulfillment of the  
Requirements for the Degree of  
Master of Science in Engineering Physics

Kelli J. Owen, B.S.  
Second Lieutenant, USAF

October 1990

Accession For	
NTIS CRA&I	<input checked="checked" type="checkbox"/>
DTIC TAB	<input type="checkbox"/>
Unannounced	<input type="checkbox"/>
Justification	
By	
Distribution /	
Availability Codes	
Dist	Avail and/or Special
A-1	

### Acknowledgments

I had a lot of support and encouragement in this research project, and the following is only a small note for my enormous appreciation of this support.

First and foremost, a special, sincere thanks goes to my advisor and teacher, Dr. Luke, for his dedication to helping me learn and his unending patience. I would also like to thank Major Lange for his time and instruction.

I have found that the people from whom I have asked for information and help, primarily the WPAFB Staff Meteorologists and the AFGL LOWTRAN7 experts, are extremely willing to take time to help in whatever way they can. I would like to give a special thanks to Mrs. Sandra Weaver for her willingness to spend time with me learning LOWTRAN7 and seeking answers to the multitude of questions that arose. My introduction to the Air Force has been extremely positive from observing the sincere dedication of all the aforementioned people.

Last, but not by any means least, I could not have accomplished this project without the loving support of my family and friends. I cannot express enough appreciation to Mom (who now is almost fluent in Greek), Dad, Bryan, Lori, and my wonderful Ryan, who have sat with me at the keyboard, listened to me on the phone, and travelled many miles to share supportive hugs, smiles, and unending encouragement.

Kelli J. Owen

## Table of Contents

	Page
Acknowledgments . . . . .	ii
List of Figures. . . . .	v
List of Tables . . . . .	viii
Abstract . . . . .	ix
I. Introduction . . . . .	1
II. Background . . . . .	5
Detection Systems and Radiometric Calculations . . . . .	5
General Detection Systems . . . . .	6
Imaging System . . . . .	6
Non-Imaging System . . . . .	8
General Radiometry . . . . .	10
Figures-of-Merit Calculations . . . . .	14
Contrast . . . . .	14
Change in Signal (CS) . . . . .	14
Single and Multiple Scattering . . . . .	17
LOWTRAN7 . . . . .	19
General Information . . . . .	19
LOWTRAN7 Outputs . . . . .	20
Transmittance . . . . .	21
Description . . . . .	21
Calculations . . . . .	21
Radiance . . . . .	23
Description . . . . .	23
Calculations . . . . .	29
Overview . . . . .	32
III. Scenarios and Calculation Methods . . . . .	33
Scenarios . . . . .	33
Calculation Methods. . . . .	35
IV. System 1: An Imaging System . . . . .	40
Contrasts . . . . .	40
General Results . . . . .	41
Varying Background Emissivity . . . . .	42
Varying Boundary Layer Aerosols (IHAZE). . . . .	44
Varying Atmospheric Profiles (MODEL). . . . .	47
Varying Relative Humidity . . . . .	50
Varying Absolute Humidity . . . . .	52
InSb vs. PtSi . . . . .	53

V.	System 2: A Non-Imaging System . . . . .	55
	General Results . . . . .	57
	Varying Background . . . . .	58
	Varying Boundary Layer Aerosols (IHAZE), Atmospheric Profiles (MODEL), and Relative Humidity . . . . .	60
	InSb vs. PtSi . . . . .	60
VI.	Single and Multiple Scattering . . . . .	61
	SALB . . . . .	61
	Aerosols . . . . .	63
VII.	Conclusions and Recommendations . . . . .	67
	Appendix A: Input Parameters . . . . .	A1
	Appendix B: Sources of Information . . . . .	B1
	Appendix C: Figures and Tables of Data . . . . .	C1
	Appendix D: Terms and Definitions . . . . .	D1
	Bibliography . . . . .	100

# List of Figures

Figure 1	AN IMAGING SYSTEM . . . . .	6
Figure 2	A NON-IMAGING SYSTEM . . . . .	9
Figure 3	GENERAL DETECTION SYSTEM SCENARIO . . . . .	10
Figure 4	SUMMATION OF AVERAGE TRANSMITTANCES. . . . .	22
Figure 5	ATMOSPHERIC RADIANCE . . . . .	24
Figure 6	SINGLE SCATTERED PATH RADIANCE . . . . .	27
Figure 7	MULTIPLE SCATTERED PATH RADIANCE . . . . .	27
Figure 8	GROUND REFLECTED RADIANCE, DIRECT AND INDIRECT .	28
Figure 9	ATMOSPHERIC PATH . . . . .	30
Figure 10	SCENARIO 1 . . . . .	33
Figure 11	SCENARIO 2 . . . . .	35
Figure 12	$\eta(\lambda) * \lambda$ VS WAVELENGTH FOR PtSi . . . . .	36
Figure 13	TARGET, BACKGROUND, AND PATH EFFECTIVE RADIANCES CALCULATED BY LOWTRAN7, SCENARIO 1 . . . . .	37
Figure 14	SCR'S FOR DAYTIME, SCENARIO 1, PtSi DETECTOR . .	38
Figure 15	TRANSMITTANCE VS. WAVELENGTH FOR SEVERAL ATMOSPHERIC CONSTITUENTS, AND TOTAL SPECTRAL TRANSMITTANCE, SCENARIO 1 . . . . .	39
Figure 16	SCALED COUNT RATES (SCRs) FOR DAYTIME, SCENARIO 1, VEGETATION BACKGROUND, HgCdTe DETECTOR . . . . .	43
Figure 17	AVERAGE CONTRAST OVER THE 3.3-4.2 $\mu$ m BAND FOR EACH BOUNDARY LAYER AEROSOL (IHAZE), InSb DETECTOR, SCENARIO 2 . . . . .	45
Figure 18	AVERAGE CONTRAST OVER THE 3.3-4.2 $\mu$ m BAND FOR EACH BOUNDARY LAYER AEROSOL (IHAZE), PtSi DETECTOR, SCENARIO 2 . . . . .	46
Figure 19	AVERAGE CONTRAST OVER THE 8-12 $\mu$ m BAND FOR EACH BOUNDARY LAYER AEROSOL (IHAZE), HgCdTe DETECTOR, SCENARIO 2 . . . . .	46

Figure 20	AVERAGE CONTRAST OVER THE 3.3-4.2 $\mu$ m BAND FOR EACH ATMOSPHERIC PROFILE (MODEL), InSb DETECTOR, SCENARIO 2 . . . . .	48
Figure 21	AVERAGE CONTRAST OVER THE 3.3-4.2 $\mu$ m BAND FOR EACH ATMOSPHERIC PROFILE (MODEL), PtSi DETECTOR, SCENARIO 2 . . . . .	49
Figure 22	AVERAGE CONTRAST OVER THE 8-12 $\mu$ m BAND FOR EACH ATMOSPHERIC PROFILE (MODEL), HgCdTe DETECTOR, SCENARIO 2 . . . . .	49
Figure 23	InSb RESPONSIVITY VS. WAVELENGTH . . . . .	54
Figure 24	BLACKBODY RADIANCE TIMES EMISSIVITY VS. WAVELENGTH . . . . .	57
Figure 25	SCR EVALUATED AT 3.802 $\mu$ m, InSb DETECTOR, DAY . . .	61
Figure 26	LOWTRAN7 GEOMETRY . . . . .	A10
Figure 27	THE LEN OPTION . . . . .	A11
Figure C1	SCRs FOR NIGHTTIME, SCENARIO 1, VEGETATION BACKGROUND, HgCdTe DETECTOR . . . . .	C1
Figure C2	SCRs FOR DAYTIME, SCENARIO 1, SNOW BACKGROUND, HgCdTe DETECTOR . . . . .	C1
Figure C3	SCRs FOR NIGHTTIME, SCENARIO 1, SNOW BACKGROUND HgCdTe DETECTOR . . . . .	C2
Figure C4	SCRs FOR DAYTIME, SCENARIO 1, VEGETATION BACKGROUND, InSb DETECTOR . . . . .	C2
Figure C5	SCRs FOR NIGHTTIME, SCENARIO 1, VEGETATION BACKGROUND, InSb DETECTOR . . . . .	C3
Figure C6	SCRs FOR DAYTIME, SCENARIO 1, VEGETATION BACKGROUND, PtSi DETECTOR . . . . .	C3
Figure C7	SCRs FOR NIGHTTIME, SCENARIO 1, VEGETATION BACKGROUND, PtSi DETECTOR . . . . .	C4
Figure C8	SCRs FOR DAYTIME, SCENARIO 1, SNOW BACKGROUND, InSb DETECTOR . . . . .	C4
Figure C9	SCRs FOR NIGHTTIME, SCENARIO 1, SNOW BACKGROUND, InSb DETECTOR . . . . .	C5
Figure C10	SCRs FOR DAYTIME, SCENARIO 1, SNOW BACKGROUND, PtSi DETECTOR . . . . .	C5



Figure C11	SCRs FOR NIGHTTIME, SCENARIO 1, SNOW BACKGROUND, PtSi DETECTOR . . . . .	C6
Figure C12	SCR EVALUATED AT 3.802 $\mu$ m, PtSi DETECTOR, DAY . .	C7
Figure C13	SCR EVALUATED AT 4.00 $\mu$ m, InSb DETECTOR, NIGHT .	C8
Figure C14	SCR EVALUATED AT 3.509 $\mu$ m, PtSi DETECTOR, NIGHT .	C8
Figure C15	SCR EVALUATED AT 8.511 $\mu$ m, HgCdTe DETECTOR, DAY .	C9

## List of Tables

<u>Table</u>	<u>Page</u>
1. Applicable Detector Materials . . . . .	5
2. The Effect of Increasing SALB on Radiance Calculations . . . . .	29
3. Day and Night Contrasts with Vegetation and Snow Backgrounds . . . . .	44
4. Boundary Layer Aerosols Tested . . . . .	45
5. Atmospheric Models Tested . . . . .	47
6. Average CS Calculated Using Different Variables in Scenario 2, in the 3.3-4-2 and the 8-12 $\mu$ m Wavebands . . . . .	56
7. Transmitted Radiances for Vegetation and Snow Backgrounds Obtained from LOWTRAN7 at 4 $\mu$ m . . . . .	59
8. Multiple Scattering Effects on Contrast Calculations Using Scenario 1 . . . . .	64
9. Multiple Scattering Effects on CS Calculations Using Scenario 2 . . . . .	65
C1. Average Contrasts (%) Calculated When Varying Relative Humidity in Scenario 1 . . . . .	C6
C2. Average Contrasts (%) Calculated When Varying Absolute Humidity in Scenario 1 . . . . .	C7

### Abstract

The purpose of this study is to demonstrate how the LOWTRAN7 computer model can be used for detection system design and analysis. The LOWTRAN7 code is an atmospheric model that performs low resolution calculations ( $20\text{cm}^{-1}$  bandwidth) to estimate atmospheric transmittance and radiance under a given set of conditions.

Generic imaging and non-imaging systems are analyzed. A hypothetical figure-of-merit is evaluated for each type of system using the transmittance and radiance calculated by LOWTRAN7. The figure-of-merit calculated for the imaging system is contrast, the difference between the target and background input signals divided by the target input signal. The figure-of-merit evaluated for the non-imaging system is the change in signal (CS), the difference between the input signal with the target in the field-of-view and the input signal without the target in the field-of-view divided by the input signal without the target in the field-of-view.

Changing atmospheric, target, and background characteristics in LOWTRAN7 has different effects on the figures-of-merit. The characteristics tested are: background emissivity, target temperature, boundary layer aerosols, atmospheric profiles, relative humidity, and absolute humidity. Two different sensor-target geometries using different paths are studied. Unexpected effects due to multiple scattering are found.

THE USE OF THE LOWTRAN7  
ATMOSPHERIC TRANSMITTANCE AND RADIANCE  
COMPUTER PROGRAM FOR DETECTION  
SYSTEM DESIGN AND ANALYSIS

I. Introduction

The purpose of an electro-optic system is to discriminate, recognize, or identify a target from other sources in its field-of-view. Atmospheric conditions can significantly influence how well a system can perform such missions. A key consideration in the evaluation or design of a system is the extent to which the atmosphere affects its ability to discriminate a target. The LOWTRAN7 computer program is an atmospheric model that calculates transmittance and radiance for a given set of conditions. The purpose of this project is to demonstrate how LOWTRAN7 may be used in system analysis and design to determine a system's effectiveness under a given set of atmospheric conditions.

An electro-optic system can be modelled as a single equivalent lens and a detector plane. The lens focuses radiation onto the detector or detector array, which produces an electrical output proportional to the incident radiation. The types of detector materials used in this study are Indium Antimonide (InSb), Platinum Silicide (PtSi), and Mercury-Cadmium-Telluride (HgCdTe). There are two general types of systems considered in this paper: an imaging system, which

utilizes an array of detectors, and a non-imaging system, which utilizes a single detector.

To describe a system's efficiency in performing a desired task, some aspect of its performance must be measured under a given set of conditions. This measured parameter will be referred to as the system's figure-of-merit. Figures-of-merit are used to compare the performance of similar systems. Typically, the signal to noise ratio (S/N) is used as a system figure-of-merit, frequently in the form of a noise equivalent parameter. Noise is not considered in this study. Rather, simpler figures-of-merit are used to demonstrate the influence of the atmosphere on each system's ability to discriminate a target and to allow a comparison of the different detector materials utilized. The two figures-of-merit used in this study are not all that must be considered when analyzing a detection system. Other figures-of-merit give different information about the capabilities of the system. For the purposes of this study, however, only one figure-of-merit for each system is calculated and examined.

An integral part of designing a system or analyzing its performance is being able to estimate the influence of the atmospheric conditions. The following picture will be considered. A detection system is aimed toward a target. Both are positioned in some geometry relative to the earth and each other. Many sources of radiation are in the system's field-of-view. First, thermal emission from the boundary,

(whatever is at the end of the path, which could be a target, background, cloud, atmospheric layer, etc.), is present. The target produces the signal the system is looking for, and the background signal is produced by anything in the target plane surrounding the target. The backgrounds used in this study are vegetation and snow and they are assumed to be uniform. Thermal emission also comes from the particles that lie in the path between the boundary and the sensor. Second, the system will "see" solar or lunar radiation that is scattered from the boundary and scattered from the particulate in the path. The radiation from any of these sources may scatter into or out of the path; if the atmospheric particle density is high, the radiation will very likely be scattered more than once. (Scattering is analogous to colliding billiard balls, and results in a redirection of the colliding radiation. The more billiard balls are present, the more collisions will occur). All of the previously mentioned sources of radiation are spectral, that is, they vary depending on wavelength.

As the various beams of radiation travel through the atmosphere, their characteristics are distorted by their encounters with atmospheric constituents, causing emission, scattering, and absorption. The fraction of radiation from any point in space that reaches any other point in space is the transmittance. The transmittance depends on the particular atmospheric path, and what lies in the path. It is also a spectral quantity.

The LOWTRAN7 computer code may be operated in one of two primary modes to calculate radiation and transmittance. The output of the first mode is the separate spectral transmittance through the atmospheric constituents and the total spectral transmittance. The second mode estimates the total spectral transmittance, as well as the amount of reflected radiation from the boundary, thermal radiation from the boundary, scattered radiation from the path, and thermal radiation from the path that reaches the electro-optic system (sensor). The radiation is reported in terms of an equivalent spectral radiance. The program has a low resolution ( $20\text{ cm}^{-1}$ ) and is therefore useful only for broadband applications.

This project illustrates how to obtain radiance and transmittance information from the LOWTRAN7 computer model and use it in generic system design and analysis problems. Prudent assumptions necessary for program utilization are discussed. Some detection system analysis is performed, the methods used are reported, and general trends found are discussed to indicate the kinds of information the user can obtain from this type of analysis.

## II. Background

This chapter gives background information about detection systems, radiometry, and the LOWTRAN7 computer model.

### A. Detection Systems and Radiometric Calculations

There are two generic types of detection systems that are used in this project: an imaging system and a non-imaging system. In the infrared, the 3-5 $\mu\text{m}$  and the 8-12 $\mu\text{m}$  bands are used in detection systems because they are atmospheric transmission windows. Three of the most popular detector materials used are shown in Table 1 (1). Each of these is employed in this study to demonstrate how program information helps determine each material's strengths and weaknesses in different situations.

Table 1  
Applicable Detector Materials

<u>Material</u>	<u>Band Used</u>	<u>Typical Quantum Efficiency</u>
InSb	3-5 $\mu\text{m}$	$\eta = 0.65$
PtSi	3-5 $\mu\text{m}$	$\eta(\lambda) = 0.31(1-0.169\lambda)^2 hc/e\lambda$
HgCdTe	8-12 $\mu\text{m}$	$\eta = 0.50$

The following is a description of the imaging and non-imaging systems, and the figures-of-merit used for each. Radiometric calculations used to evaluate signals produced in



detection systems (including the dependence of the signal on the detector material used) are explained. Using knowledge about the system and knowledge of radiometry, the specific figures-of-merit calculations are developed.

i. General Detection Systems.

a. Imaging System.

The generic imaging system is composed of a lens and two or more detectors (an array), as shown in Figure 1. Each detector "sees" one segment of the whole picture, which is called an instantaneous field-of-view. The primary assumption made is that the target is large compared to the instantaneous field-of-view.

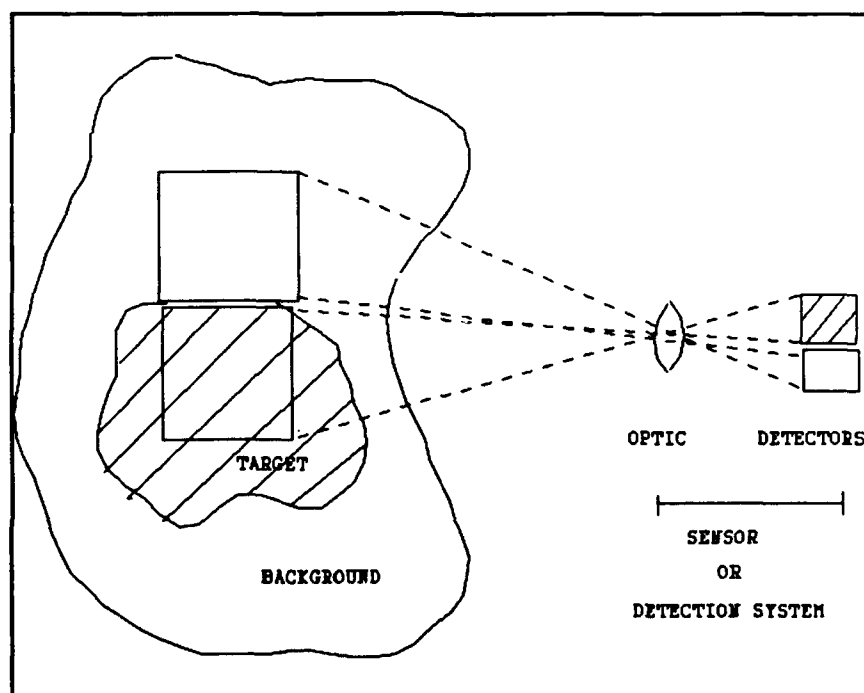


Figure 1 AN IMAGING SYSTEM

If the radiance from the target, (a particular object in the field-of-view), is different than the radiance from the background, (whatever is in the target plane besides the target), and the target is large compared to the instantaneous field-of-view, then the current output from the detector that sees the target will be different from that of the detector that sees the background. The larger the difference between the radiances, the easier it is to discriminate a target. There are other terms that contribute to the radiance incident on the detector, thereby contributing to the output signal. Two other terms that are calculated in LOWTRAN7 and used in this study are the solar radiance scattered by the particles in the path and the thermal radiance emitted by the particles in the path. The contribution from these terms is the same for any side-by-side detectors.

It is assumed, then, that one detector's footprint (the footprint refers to the area of the target-background plane in the detector's field-of-view) covers only target material and another detector's footprint covers only background material (see Figure 1). The output of the first detector is caused by target reflected, target thermal, path scattered, and path thermal radiances. The output of the second detector is caused by background reflected, background thermal, path scattered, and path thermal radiances. The two output signals from the detectors can be compared to see how much difference there is between them.

Figures-of-merit describe how well a detection system can perform the task of discrimination. A figure-of-merit that can be used in the comparison discussed above is contrast. For this study, contrast is defined as follows:

$$\text{Contrast} = \left| \frac{\text{Signal}_{\text{tg+path}} - \text{Signal}_{\text{bg+path}}}{\text{Signal}_{\text{tg+path}}} \right| \quad \text{Eq (1)}$$

where signal refers to the output signal of the detector. (From this point forward "target" (tg) will include both target thermal and target reflected radiance unless otherwise indicated. The same will be true for "background" (bg). "Path" will include path thermal and path scattered radiance unless otherwise indicated). The contrast may be negative if the target signal is less than the background signal; but as indicated in Equation 1, all contrasts are reported as absolute values for the purposes of this paper. The evaluation of the output signal is discussed in the next section.

b. Non-Imaging System.

A non-imaging system consists of a lens and one detector (see Figure 2). The primary assumption made for this system is that the target is small compared to the field-of-view (as opposed to the large target - footprint ratio assumed for the previous system). The way the system determines if a particular target is present is that the target radiation adds (or subtracts) enough radiation to the total background

radiation that it is apparent that something else is in the field-of-view.

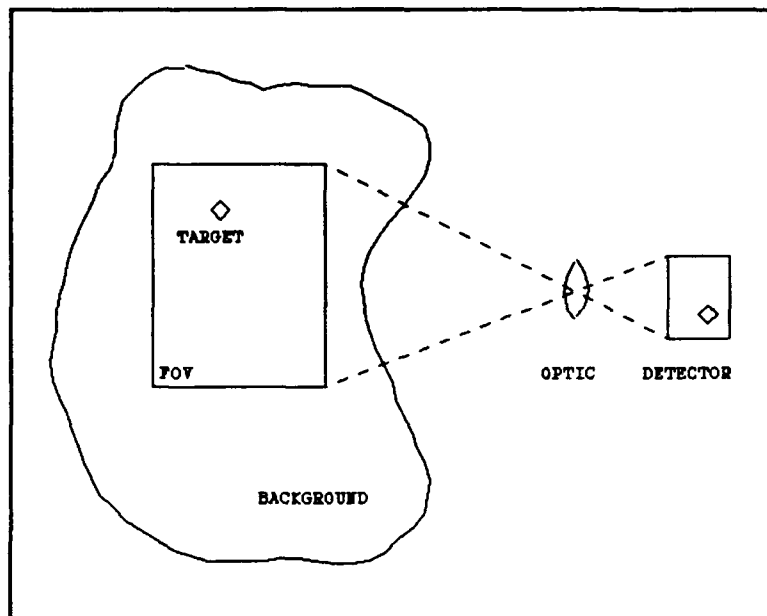


**Figure 2 A NON-IMAGING SYSTEM**

When a target enters the field-of-view of a non-imaging system, the output of the sensor changes because the strength of the radiation from the entire field-of-view changes. With no target present, the output signal is due to a sum of the following: the background emitted radiance, the background reflected radiance, the path thermal radiance, and the path scattered radiance. When the target is completely in the field-of-view, the output signal is a sum of the following: the fraction of the background emitted and reflected radiance that is not blocked by the target, the target thermal and reflected radiance, the path thermal radiance, and the path scattered radiance. The output signal for each situation may

be calculated and the difference between them reported as the change in signal (CS):

$$CS = \frac{Signal_{bg+tg+path} - Signal_{bg+path}}{Signal_{bg+path}} \quad \text{Eq (2)}$$

where "signal" is the output signal of the detector. This is the figure-of-merit used for the non-imaging system in this study.

Before specific contrast and CS equations are shown, some basic radiometric calculations of output signals will be described.

#### ii. General Radiometry.

To evaluate the previously mentioned output signals and figures of merit, the following assumptions and equations are used. The scenario is set up as follows:

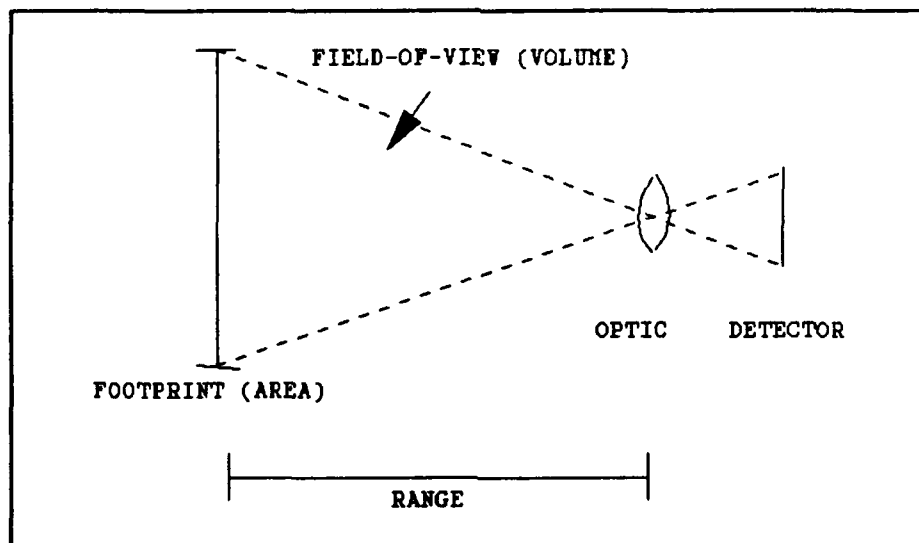


**Figure 3** GENERAL DETECTION SYSTEM SCENARIO

The optic transmittance is assumed to be non-spectral. The field-of-view is the cone of space that the sensor "sees", defined as

$$\Omega_{FOV} = \frac{A}{R^2} \quad \text{Eq (3)}$$

where

A is the area subtended on a sphere of radius R, or the area of the target-background plane that the system sees if the viewing angle is small (footprint)

R is the range from the optic to the source

The target radiance within the field-of-view is assumed to be uniform over the target. Far field approximations are also made. From the knowledge of the irradiance incident onto the optic, the relationship between power and irradiance, and neglecting refraction effects, the current produced from the detector by radiation from the instantaneous field-of-view is

$$i(\lambda) = A_o \Omega_{FOV} \tau_o \int_{\lambda_1}^{\lambda_2} R(\lambda) L(\lambda) \tau(\lambda) d\lambda \quad \text{Eq (4)}$$

where

$A_o$  is the area of the optic

$\Omega_{FOV}$  is the field-of-view

$\tau_o$  is the transmittance of the optic

$R(\lambda)$  is the responsivity of the detector

$L(\lambda)$  is the radiance from all of the sources in the field-of-view, including the path (assumed uniform over the field-of-view)

$\tau(\lambda)$  is the atmospheric transmittance

If there is a uniform target in the field-of-view which is small compared to the whole field-of-view, the output signal produced by it is

$$i_{tg}(\lambda) = \frac{A_o \tau_o A_s}{R^2} \int_{\lambda_1}^{\lambda_2} L_{tg}(\lambda) \tau(\lambda) R(\lambda) d\lambda \quad \text{Eq (5)}$$

where

$A_s$  is the projected target area in the line of sight

$R$  is the range to the target

$L_{tg}(\lambda)$  is the radiance from the target

(This is assuming no path contribution, which is not necessarily a realistic assumption.)

The current integral of Equation 5 may be expressed another way. For a Lambertian blackbody

$$M(\lambda) = \pi L(\lambda) \quad \text{Eq (6)}$$

The ideal photovoltaic photon detector responsivity,  $R(\lambda)$ , is related to its quantum efficiency by the relation

$$R(\lambda) = \frac{e\eta(\lambda)\lambda}{hc} \quad \text{Eq (7)}$$

where

$$e = 1.6022 \times 10^{-19} \text{C (electron charge)}$$

$$h = 6.6261 \times 10^{-34} \text{Js (Planck's constant)}$$

$$c = 2.9979 \times 10^{14} \mu\text{m/s (speed of light)}$$

By substituting Equations 6 and 7 into Equations 4 and 5, the output current can be expressed in terms of a parameter called the scaled count rate (SCR):

$$i_{bg}(\lambda) = \frac{\tau_o A_o \Omega_{fov} e}{hc\pi} SCR(\lambda) \quad \text{Eq (8)}$$

and

$$i_{tg}(\lambda) = \frac{\tau_o A_o A_s e}{hc\pi R^2} SCR(\lambda) \quad \text{Eq (9)}$$

The SCR is defined as

$$SCR = \int_{\lambda_1}^{\lambda_2} SCR(\lambda) d\lambda = \int_{\lambda_1}^{\lambda_2} M(\lambda) \tau(\lambda) \eta(\lambda) \lambda d\lambda \quad \text{Eq (10)}$$

where

$\eta(\lambda)$  is the quantum efficiency of the detector at the wavelength of interest

$\tau(\lambda)$  is the atmospheric transmittance from the target to the detection system

$M(\lambda)$  is the spectral exitance (2)

The SCR is analogous to the current output of the detector; however, instead of being a measurement of current, it is a



count of the photoexcited electrons in the detector when the radiation is incident upon it.

### iii. Figures-of-Merit Calculations.

Now that methods of calculating the signal are known, the figures-of-merit are specifically calculated as follows.

#### a. Contrast.

Two values must be known to calculate the contrast:

- 1) The SCR of the detector that "sees" only the background

$$SCR_{c1} = \pi \int_{\lambda_1}^{\lambda_2} (L_{path}(\lambda) + L_{bg}(\lambda)) \eta(\lambda) \tau(\lambda) \lambda d\lambda \quad \text{Eq (11)}$$

- 2) The SCR of the detector that "sees" only the target

$$SCR_{c2} = \pi \int_{\lambda_1}^{\lambda_2} (L_{path}(\lambda) + L_{tg}(\lambda)) \eta(\lambda) \tau(\lambda) \lambda d\lambda \quad \text{Eq (12)}$$

The contrast is then:

$$\text{Contrast} = \left| \frac{SCR_{c1} - SCR_{c2}}{SCR_{c2}} \right| \quad \text{Eq (13)}$$

#### b. CS.

In the non-imaging system, the target is assumed to be much smaller than the footprint of the detector. The ratio of

the output signal produced by the target to the output signal produced by the whole field-of-view when the target is not present--assuming that the background fills the footprint area--is given by

$$\frac{tg\ Signal}{whole\ Signal} = \frac{\frac{A_s}{R^2} SCR_{tg+path}}{\Omega_{FOV} SCR_{bg+path}} \quad Eq\ (14)$$

where

$A_s$  is the projected target area

$A_{fp}$  is the footprint area

Since  $\Omega_{FOV} = A_{fp}/R^2$ , and  $R$  is assumed constant (the target and background lie in the same spherical surface about the sensor), the above ratio is given by

$$\frac{tg\ Signal}{whole\ Signal} = \frac{A_s SCR_{tg+path}}{A_{fp} SCR_{bg+path}} \quad Eq\ (15)$$

It is assumed for this study that the target area is 1% of the footprint area:

$$\frac{A_s}{A_{fp}} = 0.01 \quad Eq\ (16)$$

Based on this assumption, the fraction of the area of the background that contributes to the signal when the target is in the field-of-view is 0.99.

When evaluating the CS, two values for the signal must be calculated.

- 1) The SCR when the target is not in the field-of-view

$$SCR_{cs1} = \pi \int_{\lambda_1}^{\lambda_2} (L_{bg \text{ thrm}}(\lambda) + L_{bg \text{ refl}}(\lambda) + L_{path \text{ scat}}(\lambda) + L_{path \text{ thrm}}(\lambda)) \eta(\lambda) \tau(\lambda) \lambda d\lambda \quad \text{Eq(17)}$$

The radiance contributions are thermal and reflected background radiances, and path scattered and path thermal radiances.

- 2) The SCR when the target is in the field-of-view

$$\begin{aligned} SCR_{cs2} = & \pi \int_{\lambda_1}^{\lambda_2} (L_{path \text{ thrm}}(\lambda) + L_{path \text{ scat}}(\lambda)) \eta(\lambda) \tau(\lambda) \lambda d\lambda \\ & + \pi \int_{\lambda_1}^{\lambda_2} 0.01 (L_{tg \text{ thrm}}(\lambda) + L_{tg \text{ refl}}(\lambda)) \eta(\lambda) \tau(\lambda) \lambda d\lambda \quad \text{Eq (18)} \\ & + \pi \int_{\lambda_1}^{\lambda_2} 0.99 (L_{bg \text{ thrm}}(\lambda) + L_{bg \text{ refl}}(\lambda)) \eta(\lambda) \tau(\lambda) \lambda d\lambda \end{aligned}$$

The first term in Equation 18 is the path contribution from the entire field-of-view. The second term is the target contribution from 1% of the footprint area. The third term is the background contribution from 99% of the footprint area.

The CS is then

$$CS = \frac{SCR_{cs2} - SCR_{cs1}}{SCR_{cs1}} \quad \text{Eq (19)}$$

If the CS is negative, this indicates that the target's presence causes a decrease in the signal. This happens when the target signal is smaller than the signal from the background. To determine if this will be the case, one can compare the radiances of the target and background. If the target radiance is less, this will cause the CS to be negative.

According to Equations 11, 12, 17, and 18, the  $[L(\lambda) * r(\lambda)]$  term from the following sources must be known to calculate the contrast and the CS: target thermal, target reflected, background thermal, background reflected, path thermal, and path scattered. LOWTRAN7 calculates an "effective spectral radiance",  $I(\lambda)$ , or  $[L(\lambda) * r(\lambda)]$ , for each of the previously mentioned sources. This is discussed in much more detail in section B of this chapter.

#### iv. Single and Multiple Scattering.

An important consideration when estimating the figures-of-merit using the LOWTRAN7 code is multiple scattering. Scattering occurs when the electric field of an incident beam causes the bombarded particle to oscillate at the same frequency and then reradiate at that frequency. When the entire effect is considered, there is no net change in the

internal energy of the particle (3). (Absorption, on the other hand, directly changes the internal states of the particle.) In addition, when the particle density of the scatterer is low enough, it can be assumed that the reradiation will not be rescattered by any other particles. This is called single scattering. Multiple scattering occurs when the particle density is higher, and the reradiated beam hits more particles and is therefore scattered more times (3). Radiation may be scattered into or out of the path.

LOWTRAN7 gives the user a choice of a single and multiple scattering model, and the choice is dependent on the situation. For example, when looking near the sun at high noon, the path traverses relatively less atmosphere at lower altitudes than when looking near the sun at sunset, thus the particle density in the path is lower, and single scattering is a good approximation (4). Conversely, when looking through clouds or thick fogs, particle density is high; therefore, single scattering would be unacceptable, and multiple scattering should be used (4). A synopsis of when and when not to consider multiple scattering is found on page 40 and 41 of the LOWTRAN6 Technical Report (4).

Multiple scattering may degrade or improve the figure-of-merit. The multiple scattering mode takes considerably more time to run in the program, thus it is not used in the figure-of-merit analysis. However, several tests are made and discussed in Chapter 6.

## B. LOWTRAN7

### i. General Information.

To evaluate the figures-of-merit, various transmittances and radiances must be known. This section gives specific information about LOWTRAN7 including transmittance and radiance output descriptions and calculations.

The LOWTRAN7 model has evolved through more than six other versions in over a twenty-year period. It is a complex synthesis of many models and experimental data that have accumulated throughout the years. The program calculates spectral transmittance, spectral radiance, and spectral irradiance with a moderate resolution of  $20\text{cm}^{-1}$ . It performs the calculations from 0 to  $50,000\text{cm}^{-1}$  (approximately  $0.2\mu\text{m}$  to infinity). A primary assumption made is that the atmosphere is divided into 33 uniform layers: 1km thick up to 25km, 5km thick from 25 to 50km, 10km thick from 50 to 70km, and the last layer extends from 70 to 100km. The aerosols are divided into four uniform layers: 0-2km (boundary layer), 2-10km (upper troposphere), 10-30km (lower stratosphere), and 30-100km (upper atmosphere) (4).

The program used in this project is a PC version. The mainframe version was given to WPAFB staff meteorologists by AFGL. The people at WPAFB modified some of the code to make it into this particular PC version. The Tape 5-8 outputs are the same for both programs. The Tape 6 output corresponds to the .prt file in the PC version used.

At the time of the completion of this document, a letter of errata for the mainframe version was received by the author from AFGL, dated 10 September 1990. The new program had not yet been sent to Wright-Patterson AFB. Space-to-ground geometries and solar scattered radiance calculations were among the parts of the program affected.

Since the program has been routinely revised, no complete user's manual currently exists. This paper contains a lot of information about running the program, primarily in Appendix A. There are also many other sources of information that are described in Appendix B.

ii. LOWTRAN7 Outputs.

LOWTRAN7 gives the following output information for a specified set of parameters: total transmittance, transmittance of each constituent, aerosol-hydrometeor absorption, integrated absorption, atmospheric radiance, path scattered radiance, ground reflected radiance, total radiance, integrated radiance, incident solar irradiance ("solar"), transmitted solar irradiance, integrated solar irradiance, and integrated transmitted solar irradiance. Each of these quantities is given at each incremental wavelength. This project's mission, in part, is to explain clearly what the transmittance and radiance outputs mean and how they can be best utilized.

a. Transmittance.

1. Description.

The transmittance terms in this program are defined as follows:

Total transmittance: the total fraction of the signal that will reach the sensor.

Transmittance of each constituent: the separate transmittances of eight different constituents as well as trace elements.

2. Calculations.

Transmittance is the fraction of the energy from the target that will reach the sensor. The LOWTRAN7 program calculates the total average transmittance across a user-specified range,  $\nu_1$  to  $\nu_2$ , by taking two averages.

The first average is the average transmittance taken over the incremental  $\Delta\nu$ , which in this program is fixed at  $20\text{cm}^{-1}$ . The program takes the average transmittance calculated over a  $20\text{cm}^{-1}$  bandwidth around a given  $\nu$ . (This is a broad  $\Delta\nu$ , compared to the narrow spectral line of a laser, for instance, but it is a moderate resolution that was chosen for this code). In this calculation, the transmittance is a function of a wavelength-dependent absorber coefficient, temperature, pressure, concentration of absorber (which determines the effective path length), and an empirical constant, which is dependent on the type of constituent (5). The program then



steps up  $20\text{cm}^{-1}$  (or a step size chosen by the user) and does the same calculation over the  $20\text{cm}^{-1}$  bandwidth (see Figure 4).

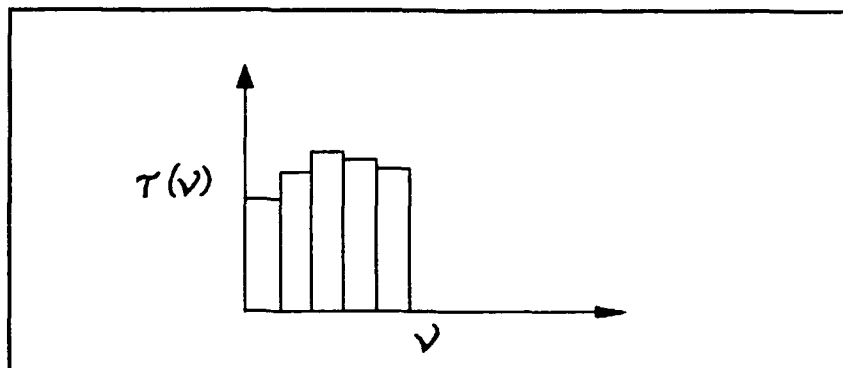


**Figure 4** SUMMATION OF AVERAGE TRANSMITTANCES

The next average is the average transmittance across the entire wavenumber range specified by the user ( $\nu_1$  to  $\nu_2$ ). The second average is determined by taking the area under the curve in the figure above, which is just an integral (or summation), and dividing it by the distance across the horizontal axis, which is the user-specified wavenumber range,  $\nu_1$  to  $\nu_2$ ; the average  $\tau$  in Figure 4 is

$$\bar{\tau}(\nu) = \frac{\int_{\nu_1}^{\nu_2} \tau(\nu) d\nu}{\nu_2 - \nu_1} \quad \text{Eq (20)}$$

(keeping in mind that each value of  $\tau(\nu)$  is itself an average over the  $20\text{cm}^{-1}$  interval).

The process is repeated for each atmospheric constituent, to achieve a final total average transmittance (5):

$$\bar{\tau}_{TOT}(\nu) = \bar{\tau}_1(\nu) * \bar{\tau}_2(\nu) * \bar{\tau}_3(\nu) * \dots \quad \text{Eq (21)}$$

In summary, the transmittance mode basically gives the spectral transmittance for each atmospheric constituent and a total spectral transmittance. The transmittance data is not necessary for the calculations in this project, because it is accounted for in the radiance calculations, as described in the next section; however, this mode is extremely useful in determining which atmospheric constituents are affecting the transmittance, thus affecting the contrast and CS, and the transmittance mode is used for that purpose in this paper.

b. Radiance.

To calculate the contrast (Equations 11 and 12) and the CS (Equations 17 and 18), the  $L(\lambda) \cdot \tau(\lambda)$  terms must be known. For each source, LOWTRAN7 actually calculates an "effective radiance",  $I(\lambda)$ , which is the radiance from the source at a given range if there was no atmosphere between the source and the sensor to affect the signal. Hence,  $I(\lambda) = L(\lambda) \cdot \tau(\lambda)$  in Equations 11, 12, 17, and 18. The  $I(\lambda)$ 's needed for the calculations are from the following sources: boundary (target and background) emission, boundary reflection, path scattering, and path emission. The following is a description of the  $I(\lambda)$  terms in LOWTRAN7 terminology, and some explanation of how they are calculated.

1. Description.

The Total Radiance calculated in the LOWTRAN7 program is a sum of three different radiances when the solar/lunar

contributions are included: the Atmospheric Radiance, the Path Scattered Radiance, and the Ground Reflected Radiance. The output lists the radiances spectrally, then gives the maximum, the minimum, and an integral sum. The following is a discussion of the Atmospheric, Path Scattered, and Ground Reflected Radiances, what they physically represent, and parameter dependencies.

Atmospheric Radiance is defined as "all thermal radiation emitted by the atmosphere or by the boundary (and thermal radiation scattered by the atmosphere or reflected by the ground)" (6). It includes all thermal radiances: radiance emitted by the boundary and the path, and thermal radiance scattered by the path and reflected by the boundary (Figure 5). It is calculated in the "radiance" and the "radiance with solar/lunar scattering" modes, and is the same value in both cases, as it does not depend on solar/lunar effects.

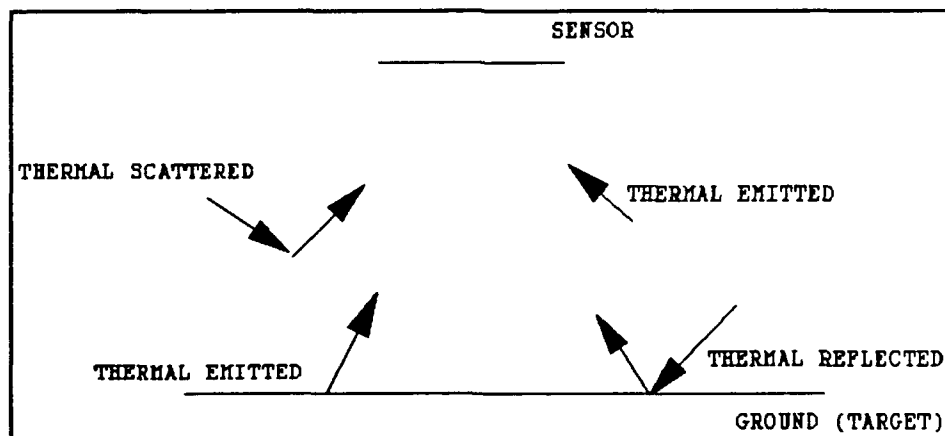


**Figure 5** ATMOSPHERIC RADIANCE

The calculation of the Atmospheric  $I(v)$ , the effective thermal radiance, depends on two inputs: SALB (surface, or

boundary, albedo) and TBOUND. TBOUND is the temperature of the boundary, which is anything at the end of the path. SALB stands for surface albedo, which is a non-spectral measure of reflectance. SALB is misleading, because actual inputs are average reflectivities over the waveband of interest. Reflectivity is a spectral quantity, as is emissivity, defined by:

$$e(\lambda) = 1 - \rho(\lambda) \quad \text{Eq (22)}$$

The reflectivity cannot be input spectrally so it is referred to as SALB. As the SALB increases, the value of the Atmospheric Radiance decreases. This is because as SALB increases, emissivity decreases, and the thermal radiance is lower with a lower emissivity. As temperature increases, the thermal radiance increases.

The Atmospheric Radiance is the sum of a path thermal radiance and a boundary thermal radiance, where the boundary (which is whatever is at the end of the path, the target, the background, an atmospheric layer, etc.), is specified by TBOUND and SALB, i.e., its temperature and average reflectivity. In some cases, such as when evaluating the CS, it is necessary to know only the path thermal radiance or only the boundary thermal radiance. The separation is made as follows. If SALB and TBOUND are set to 0, then there is no thermal radiation reflected or emitted by the boundary. The output is then only the path thermal radiance. The difference

of the sum of the path and the boundary and just the path is then the thermal radiance due only to the boundary.

When solar/lunar effects are included, two more effective radiance terms are calculated. The first is Path Scattered Radiance, which is defined as the solar radiation scattered by the atmosphere (6). Path Scattered Radiance is not at all affected by the boundary when only single scattering is considered. (Single scattering accounts for radiation scattered into the path; multiple scattering accounts for radiation scattered into or out of the path (7)). When multiple scattering is calculated, however, there is a dependence on SALB (but not TBOUND). Since more radiation is reflected from the boundary, if the boundary has a higher emissivity, path scattered radiance increases as SALB increases, as long as multiple scattering is considered. Physically the multiple scattered path radiance includes the radiation that is scattered by the atmosphere and then scattered by the ground or another particle to hit the sensor (it also accounts for the radiation that is scattered out of the path) (7). The single path scattered radiance is represented in Figure 6, and the multiply scattered path radiance is shown in Figure 7. The contribution from the radiation scattered from the ground depends on the SALB and the geometry of the situation (4).

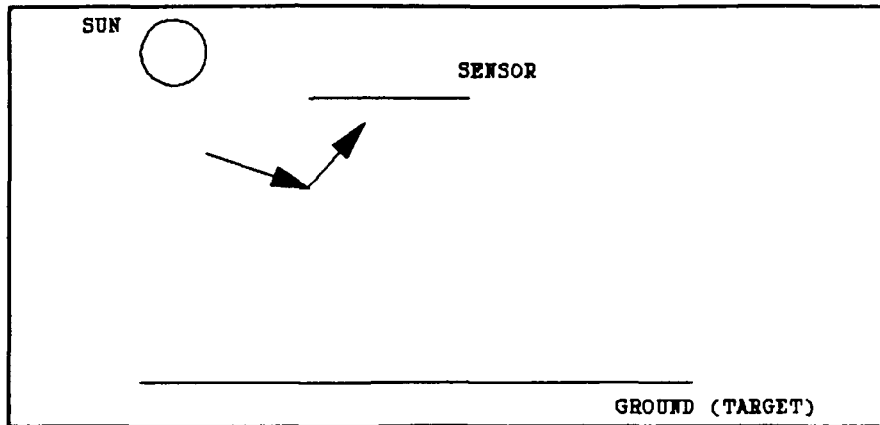


**Figure 6** SINGLE SCATTERED PATH RADIANCE

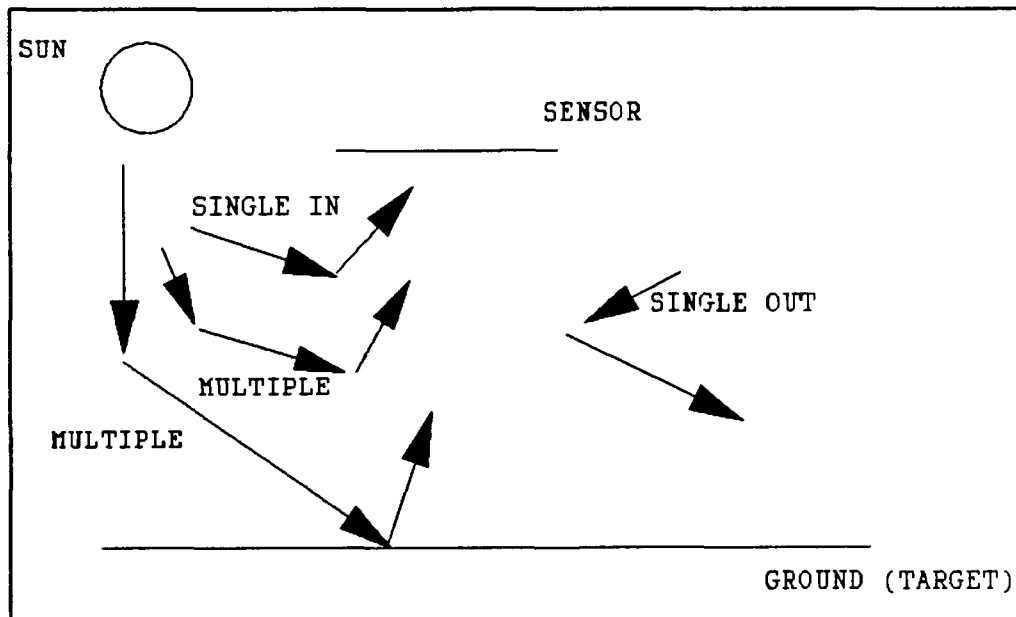


**Figure 7** MULTIPLE SCATTERED PATH RADIANCE

The final effective radiance term in the Total Radiance is the Ground Reflected Radiance. It is the solar radiation reflected by the boundary (6). It does not depend on TBOUND but it does depend on SALB (which is physically obvious - it is not emitted, just reflected). As SALB increases, Ground Reflected Radiance increases. The "direct" component is the

radiation from the sun that is reflected by the ground toward the sensor. The "indirect" component (in the output "direct" and "total", which is the sum of the direct and indirect, are given) is the solar radiation reflected by the ground then scattered by the atmospheric constituents toward the sensor (keeping in mind that the radiation can be scattered both into and out of the path if multiple scattering is used) (see Figure 8) (7) . When single scattering is used, therefore, no indirect component is calculated.

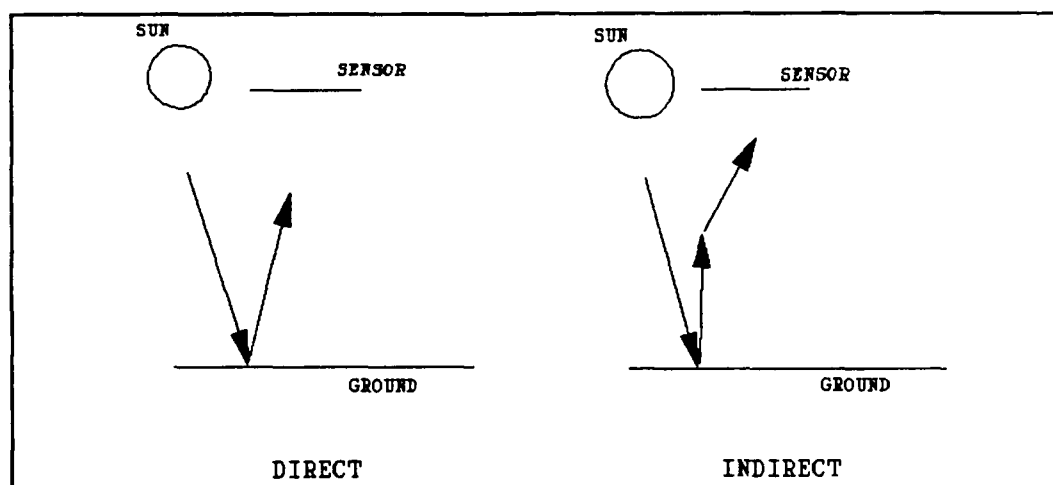


**Figure 8** GROUND REFLECTED RADIANCE, DIRECT AND INDIRECT

The Ground Reflected Radiance is not part of the path radiance at all. The indirect term is generally a small fraction of the total Ground Reflected Radiance.

Table 2 is a summary of how each type of radiance is affected by an increase in the surface albedo under the conditions tested in this paper. These results hold true in both the 3.3-4.2 and the 8-12 $\mu$ m wavebands.

Table 2

The Effect of Increasing SALB on Radiance Calculations

<u>Radiance Source</u>	<u>Single Scattered</u>	<u>Multiple Scattered</u>
Atmospheric Radiance	↓	↓
Path Scattered Radiance	-	↑
Ground Reflected Radiance	↑	↑
Total Radiance	↓	↓

At wavelengths above  $3\mu\text{m}$ , thermal contributions are dominant (at temperatures of  $298^\circ\text{K}$  used in this paper). In the 8-12 band, both the path scattered radiance and the ground reflected radiance are negligible.

All three effective radiance terms are then added to get the Total effective Radiance (given in both  $\text{Watts/cm}^2\text{-sr-}\mu\text{m}$  and  $\text{Watts/cm}^2\text{-sr-cm}^{-1}$ ).

2. Calculations.

The Atmospheric Radiance calculations are performed in a very similar manner to the transmittance calculations. Over a  $20\text{cm}^{-1}$  interval, the program calculates the average Atmospheric Radiance at the wavenumber  $\nu$  as follows (5)

$$I(\nu) = \int_{\tau_s^b}^1 d\tau_s B(\nu, T) \tau_s + B(\nu, T_b) \tau_t^t \quad \text{Eq (23)}$$

where

$I(\nu)$  is the effective radiance (see page 23)



$\bar{\tau}_a$  is the average transmittance due to absorption  
(and the differential is over one atmospheric layer)

$\bar{\tau}_s$  is the average transmittance due to scattering

$\bar{\tau}_t = \bar{\tau}_a * \bar{\tau}_s$  is the average total transmittance

$\bar{\tau}_a^b, \bar{\tau}_t^b$  is the average transmittance from the  
observer to the boundary

$B(\nu, T)$  is the Planck blackbody equation at  
temperature  $T$  and wavelength  $\nu$

$T_b$  is the temperature of the boundary (5)

A numerical representation and explanation of Equation 23  
is as follows. There are several layers of atmosphere through  
which the beam is travelling:

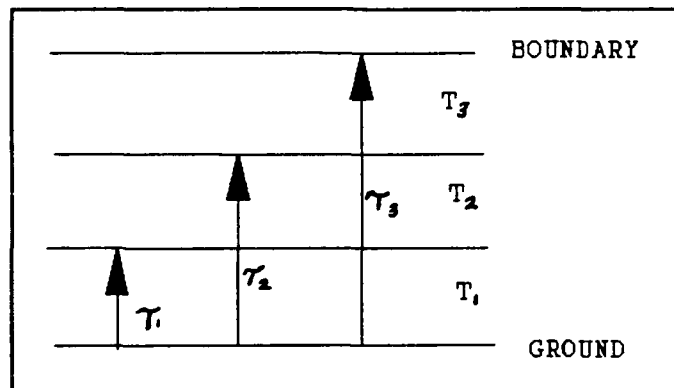


**Figure 9** ATMOSPHERIC PATH

Each layer has an average temperature ( $T_i$ ) and an average  
transmittance ( $\tau_i$ ). The first term in Equation 23 may be  
evaluated numerically as a sum of the average transmittance  
across each isothermal layer times the Planck function  
evaluated at the average temperature of that layer and a

wavenumber,  $\nu$ . The sum is added to the boundary contribution, evaluated by the second term in Equation 23. The numerical equation is

$$I(\nu) = \sum_{i=1}^{N-1} (\bar{\tau}_a(i) - \bar{\tau}_a(i+1)) B(\nu, \frac{T(i) + T(i+1)}{2}) (\frac{\bar{\tau}_s(i) + \bar{\tau}_s(i+1)}{2}) \frac{E}{q} + B(\nu, T_b) \bar{\tau}_t^b \quad (24)$$

$N$  is the number of layers and  $i$  represents each layer (8).

The first part of the equation describes the atmospheric contribution to the radiance, which includes the thermal radiation scattered by particles in the atmosphere and the thermal radiation emitted by particles in the atmosphere. The second part is the contribution of the boundary (6).  $B(\nu, T)$  is assumed to be slowly varying over  $\nu = 20\text{cm}^{-1}$ , so the average value of the radiance is approximated using the average transmittances, which are calculated by the LOWTRAN7 model over each  $20\text{cm}^{-1}$  (6). A summation (integration) of the second term is not necessary because (a) the boundary temperature is assumed constant, (b)  $B(\nu, T)$  is assumed to be varying slowly over  $\nu$ , and (c) the transmittance is already averaged.

LOWTRAN7 can calculate either the first or both terms directly (over a  $20\text{cm}^{-1}$  interval), and the second term indirectly (the user must separate the two thermal radiances as discussed above).

The next two radiances account for solar or lunar radiation. Calculations for them are more complex and are described in detail in the LOWTRAN6 Technical Report (4).

All three average terms, evaluated at the center wavenumber of a  $20\text{cm}^{-1}$  bandwidth, are then added to get an average total radiance at that wavenumber.

### C. Overview

The next three chapters explain the use of the LOWTRAN7 program, based on the information presented in the background.

Chapter 3 describes the three specific scenarios used in this project. It gives specific values for the input parameters. (More specific information about the input process is in Appendix A.) Chapter 3 also explains the methods of calculation used in this study.

Chapter 4 is an analysis of the first type of detection system - the imaging system - using the LOWTRAN7 model. It gives an analysis of the results as they are reported.

Chapter 5 is the same as chapter 4, except that a non-imaging detection system is used.

Chapter 6 is an analysis of the effect of multiple scattering on detection systems.

Chapter 7 gives conclusions and suggestions about the LOWTRAN7 program and its use, and ways to expand this study.

Appendix A is a complete description of the input process for this project. Appendix B gives sources of information. Appendix C lists data calculated throughout this study. In this paper there are many terms used, some of which have definitions specific to this paper; these are listed in Appendix D.

### III. Scenarios and Calculation Methods

#### Scenarios

In this study, two different sky-to-ground geometries are studied to demonstrate the use of LOWTRAN7. The results are reported to demonstrate what information can be obtained from this type of analysis rather than to provide specific numbers.

The following are the parameters used in the two scenarios studied. In the first scenario, the target is located on the ground at sea level, and the sensor is at a slant path of 23km at an altitude of 7km (see Figure 10). The slant path is used so that refraction effects are considered.

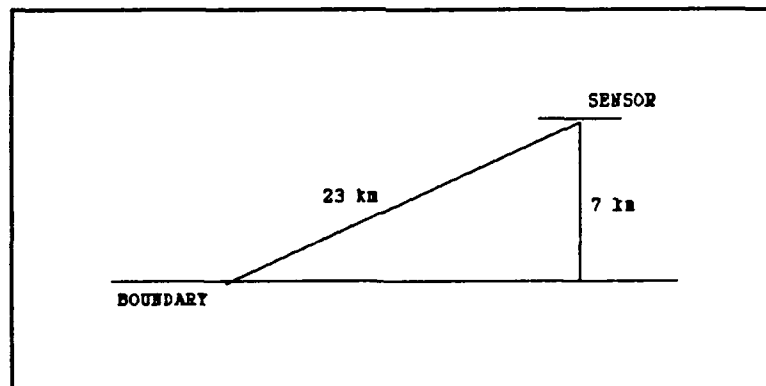


Figure 10 SCENARIO 1

The sun, in the daytime scenario, is directly over the sensor. To estimate the sun's position, the location of the target is at the equator on the prime meridian ( $0^\circ$  latitude,  $0^\circ$  longitude) at 12:00 noon Greenwich time, at approximately the day of the vernal equinox. Either equinox would suffice to provide maximum solar irradiance. At night, it is assumed

that there is no moon (or starlight, which is a very small contribution, and is not calculated in the model). In the 3.3-4.2 $\mu$ m band, InSb and PtSi detectors are used. In this portion of the 3-5 band, the transmittance and the contrast are largest (2). Hence the 3.3-4.2 band is used in this study. In the 8-12 $\mu$ m band, an HgCdTe detector is utilized. The target has a temperature of 298°K and a constant reflectivity of 0.32 across both bands (This is not a very realistic assumption. Real measurements, especially in the 8-12 band are difficult to take. When reflectivities are measured, they may be very specific, and can often only be found in classified literature). The background, whose temperature is 298°K, is an average of vegetations: grass, green coniferous twigs, and maple leaves, and the reflectivity is a function of wavelength (9). Averages of the vegetation reflectivities are taken over 5 $\mu$ m bands and then all three numbers averaged. Each final average over the 5 $\mu$ m band constitutes one value of SALB for one run over the 5 $\mu$ m band; the runs are then combined for the entire band being considered. The average reflectivity input for the vegetation varies from 0.07 to 0.17 across the 3.3-4.2 band, and from 0.04 to 0.11 across the 8-12 band (9). Snow is much more complex than a certain type of vegetation, however, and after reviewing literature by Berger and Turner, a constant value of 0.02 was chosen for both wavebands (a very rough estimate, and it is also not realistic to put snow at the equator) (9, 10).

The reflectivity of snow depends on many things, such as the time of day and the snow's density and age; for real information one must know the real situation (10). Multiple scattering is chosen for some runs in order to determine its contribution under different circumstances. A rural aerosol model with 23 kilometers meteorological range is used for the baseline. No clouds or rain are present.

In scenario 2, which is used in the non-imaging system tests, the sensor is 18 kilometers directly over the target (see Figure 11). All other parameters are the same as scenario 1 except the target temperature is 400°K.

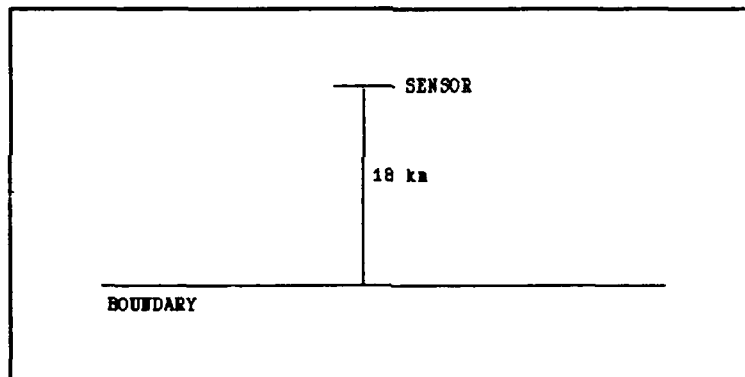


Figure 11 SCENARIO 2

#### Calculation Methods

The purpose of this section is to demonstrate how all of the previous information, the detector materials, the radiometry, the figures-of-merit, and LOWTRAN7  $I(\lambda)$  calculations, are put together to calculate average contrast and CS values.

The SCR's needed to calculate the contrast and CS, given by Equations 13 and 19, depend on 1) the  $L(\lambda) * \tau(\lambda)$ , or  $I(\lambda)$

(effective radiance) calculated by LOWTRAN7, and 2) the responsivity, or  $\eta(\lambda)*\lambda$ , of the detector material, shown in Table 1. The following is an example of how the data is put together to calculate average contrast and CS values discussed in the next three chapters.

In this example, contrast is calculated for scenario 1, daytime, using a PtSi detector in the 3-5 band. The responsivity, or  $\eta(\lambda)*\lambda$ , is shown in Figure 12.

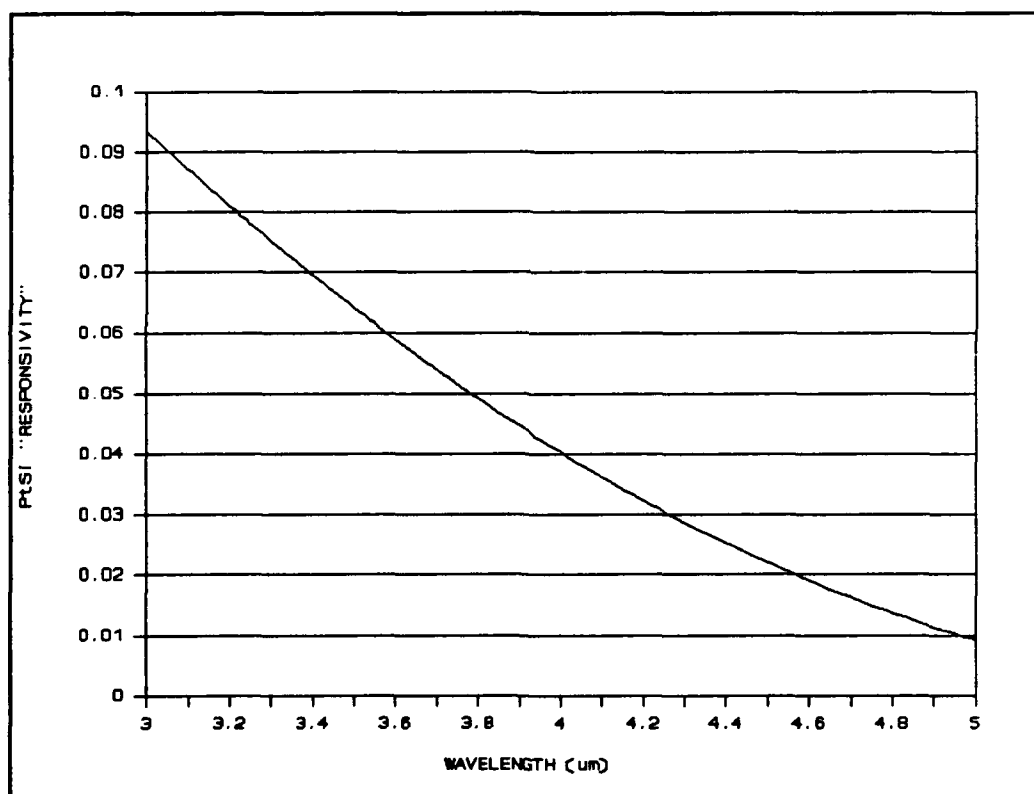
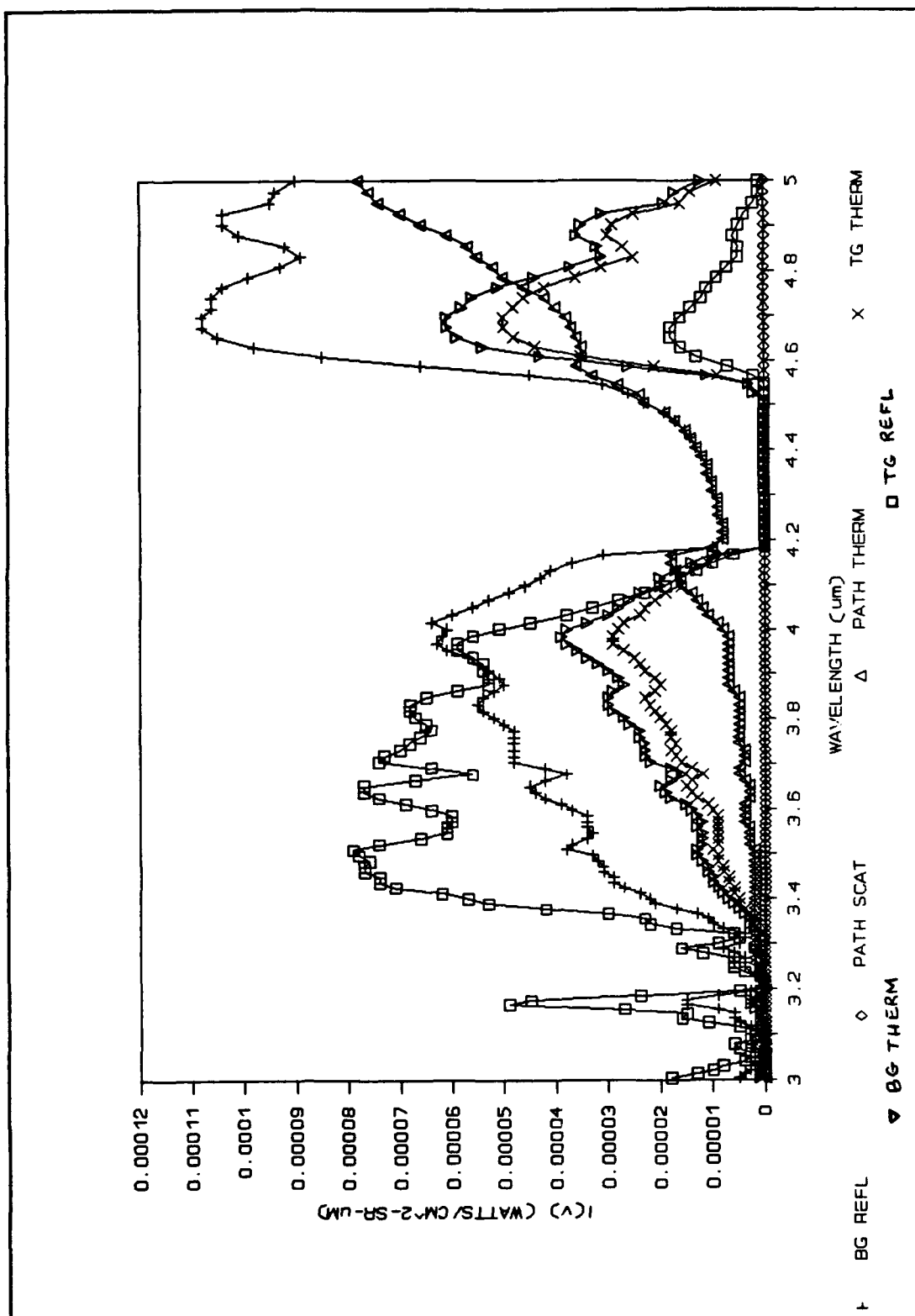


Figure 12  $\eta(\lambda)*\lambda$  VS WAVELENGTH FOR PtSi

In Figure 13, the  $I(\lambda)$  calculated by LOWTRAN7 is plotted for the following sources: target emitted and reflected, background emitted and reflected, and path emitted and scattered.



**Figure 13** TARGET, BACKGROUND, AND PATH EFFECTIVE RADIANCES CALCULATED BY LOWTRAN7, SCENARIO 1



The spectral data points in Figures 12 and 13 are multiplied to obtain the spectral SCR's for the target+path and the background+path sources (see Figure 14). The solar scattered and reflected radiances, as well as the thermal radiances, are included because this is the day scenario. If it were the night scenario, only the thermal  $I(\lambda)$ 's, or the Atmospheric Radiance values, would be included.

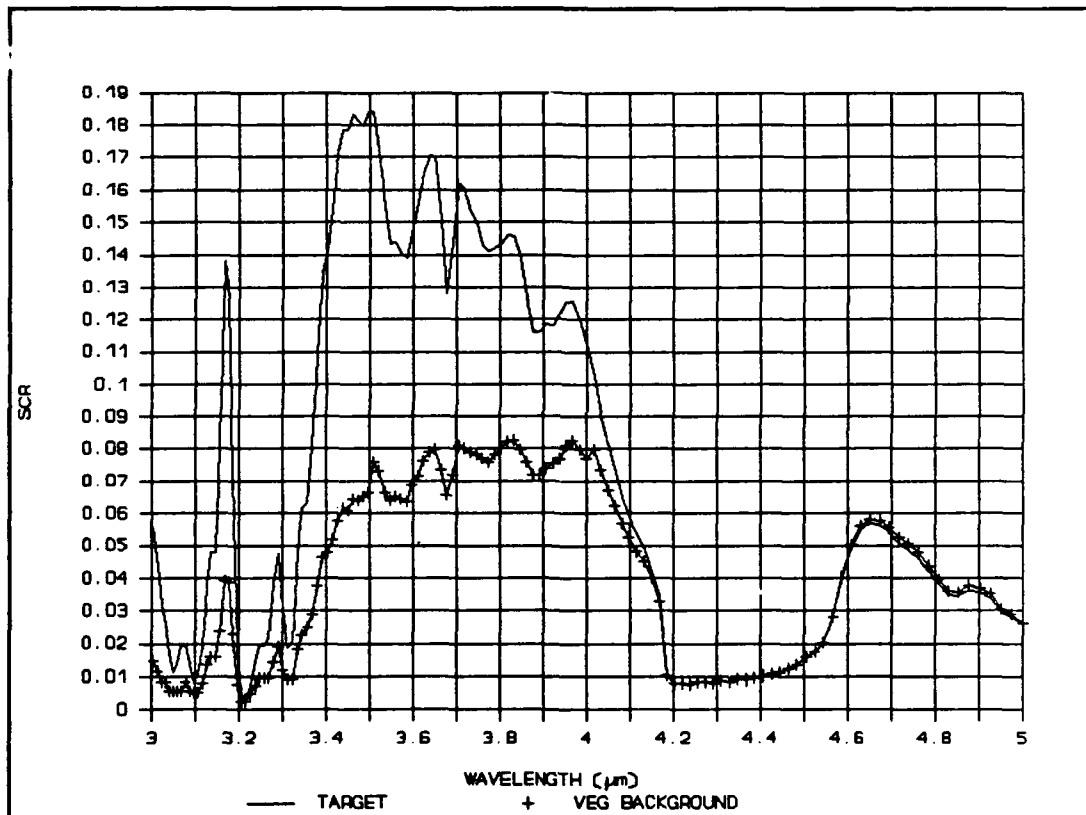


**Figure 14** SCR'S FOR DAYTIME, SCENARIO 1, PtSi DETECTOR

Equation 13 is then used to calculate the contrast, which is just the difference between the two curves divided by the value of the target curve, at each wavelength. The average, which is just a sum of those values divided by the number of values, is then calculated over the 3.3-4.2 band.

For more information about the situation, the transmittance mode is run. It calculates separate spectral transmittances for each atmospheric constituent in the program. Figure 15 shows transmittances for several constituents.

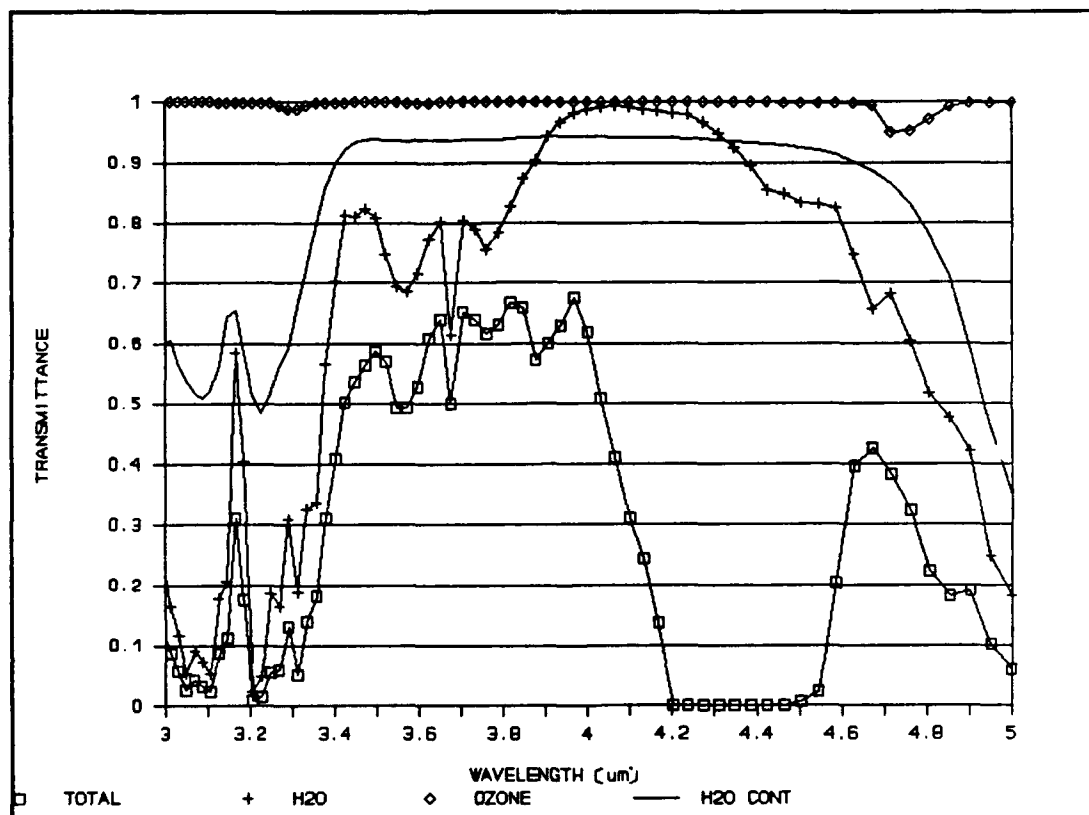


**Figure 15** TRANSMITTANCE VS. WAVELENGTH FOR SEVERAL ATMOSPHERIC CONSTITUENTS, AND TOTAL SPECTRAL TRANSMITTANCE, SCENARIO 1

From Figure 15, it can be determined which constituents are key players in transmittance degradation for a given waveband and situation. All of the previous calculations are done using a LOTUS spreadsheet to obtain the results presented in the next three chapters.

#### IV. System 1: An Imaging System

##### Contrasts

In this chapter, the contrast for an imaging system is analyzed using scenario 1. To demonstrate some of the versatility of the LOWTRAN7 program and the variety of information it can provide, the following parameters are varied: background emissivity; boundary layer aerosols; atmospheric profiles; relative humidity; and absolute humidity. Trends are analyzed and the two wavebands are compared. The final section compares the PtSi and the InSb detectors.

Before examining the contrasts, an important point should be made about the SCR, which, as previously defined, is the number of photoexcited electrons produced in the sensor by the incoming radiation. The size of the SCR varies depending on the detector material and the situation, and is an important consideration in detection system design that is not examined in this report. In the results of this paper, the magnitude of the SCR varies for the following reasons. The quantum efficiency of the PtSi detector is lower than that of the InSb in the 3-5 band by a factor of about 10, thus its SCRs are about a factor of ten smaller than the SCRs when the InSb detector is used. At higher wavelengths, since the wavelength is multiplied in the SCR equation, the SCRs may be higher in the 8-12, HgCdTe case than in the 3-5, InSb case, under

similar conditions. Another important influence on the size of the SCR is the environment. When heavy aerosols are present, for example, the transmittance decreases, thus decreasing the size of the SCR. Although this study analyzes relative SCR magnitudes rather than actual SCR magnitudes, the same methods may be used to examine SCR values.

i. General Results.

The following are general results found using scenario 1.

The background SCR is actually higher than the target SCR in all cases tested using the imaging system, except in the daytime scenario in the 3.3 to 4.2 band. The reason for this is that the sun radiates at a peak wavelength of  $0.5\mu\text{m}$ , whereas the earth's thermal radiance, at approximately  $280^\circ\text{K}$ , peaks at approximately  $10\mu\text{m}$  (11). At wavelengths above  $4\mu\text{m}$ , thermal contributions are dominant. Thermal radiance is also the dominant source of radiance at night. The amount of thermal emission is greater if the emissivity ( $\epsilon$ ) is higher (and if the temperature is higher, but temperature is not varied in the imaging system tests). The emissivity in all cases tested is higher for the background than for the target in both wavebands. The background SCR is therefore higher when thermal radiance is dominant (at night and in the 8-12 band). In the daytime in the 3.3-4.2 band, the addition of solar radiation causes the total target radiance to become greater than the total background radiance because of the target's higher reflectivity.

In the 3.3-4.2 band, the nighttime contrasts are approximately half the value of the daytime contrasts. This result is due to the difference between the target and background emissivities, their temperatures, and the addition of solar (reflected) radiance during the day. Changing any one of these variables changes this result, as is shown in the next chapter.

In the 8-12 band the day and night contrasts are basically the same, as thermal effects are completely dominant. The day and night 8-12 band contrast values match very closely the nighttime values using the InSb and PtSi detectors in the 3.3-4.2 band. This would change if target or background temperatures or emissivities changed.

ii. Varying Background Emissivity.

Two different backgrounds are tested in scenario 1: vegetation (used as a baseline throughout this study), and snow. They are assumed to have a spatially uniform temperature and emissivity. The difference between them is their reflectivity, with the vegetation having a higher average reflectivity, thus a lower emissivity, than the snow.

Figure 16 is an example of the results, showing the SCR difference between the target (temperature=298K and  $R=0.32$ , as defined in Chapter 3) and the vegetation background in the 8-12 band using an HgCdTe detector. The remaining graphs are shown in Appendix C, Figures C1, C2, and C3.

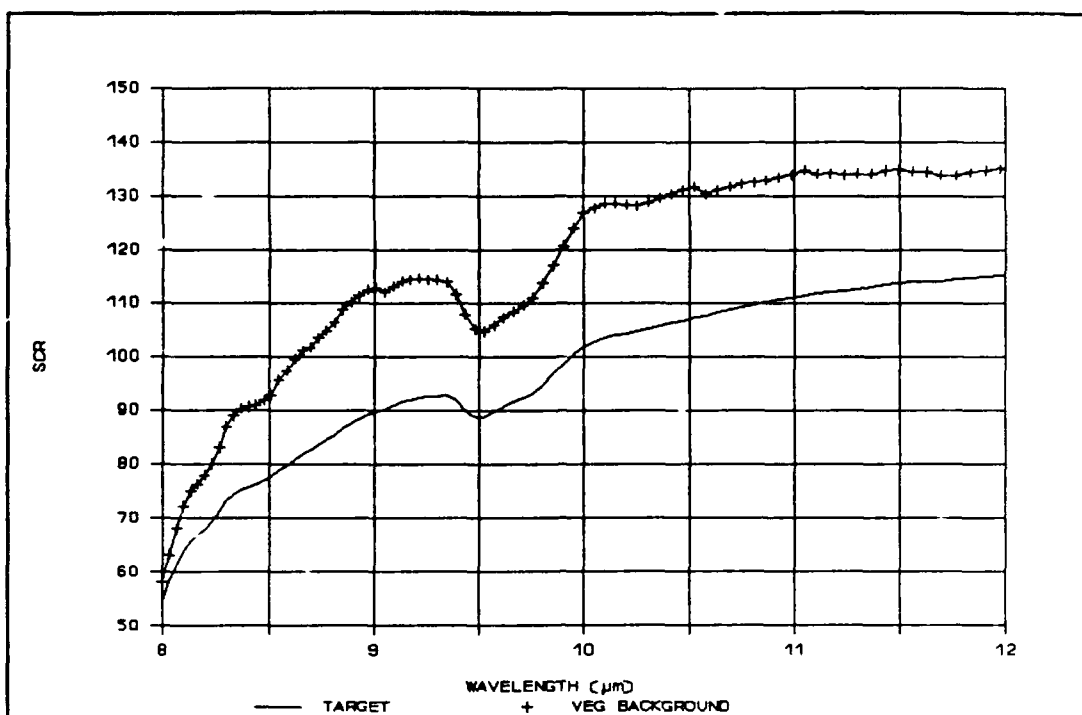


**Figure 16** SCALED COUNT RATES (SCRs) FOR DAYTIME, SCENARIO 1, VEGETATION BACKGROUND, HgCdTe DETECTOR

With the vegetation background, the average contrast is approximately 21%. With the snow background, the average contrast is approximately 25%. Since target and background temperatures are the same, the larger the difference between their emissivities, the greater the contrast.

Also shown in Appendix C, Figures C4 through C11, are the differences between targets and vegetation/snow backgrounds in the 3-5 band. Table 3 shows the average contrasts over the 3.3-4.2 band. Once again, the contrasts are greater with a snow background than with a vegetation background.

Table 3  
Day and Night Contrasts with  
Vegetation and Snow Backgrounds

<u>DAY</u>		
<u>Detector Material</u>	<u>Vegetation</u>	<u>Snow</u>
InSb	44%	59%
PtSi	51%	63%
<u>NIGHT</u>		
<u>Detector Material</u>	<u>Vegetation</u>	<u>Snow</u>
InSb	25%	31%
PtSi	25%	32%

In the daytime, when the reflected solar radiance is the larger contribution, the larger difference between the target and snow reflectivities causes the contrast to be greater than with a vegetation background. This result would be difficult to estimate, but is readily obtained from LOWTRAN7 results.

iii. Varying Boundary Layer Aerosols (IHAZE).

Another parameter that can be varied in LOWTRAN7 is the boundary layer aerosol content. Aerosols are dispersed particles in the air. In the LOWTRAN7 program, 0 to 2km is defined as the boundary layer. Different environments dictate what type of aerosol is dominant in the boundary layer. In the maritime environment, salt is an effective aerosol. In the urban environment, pollution is in the air. In the desert environment, sand is an effective aerosol (and there is more

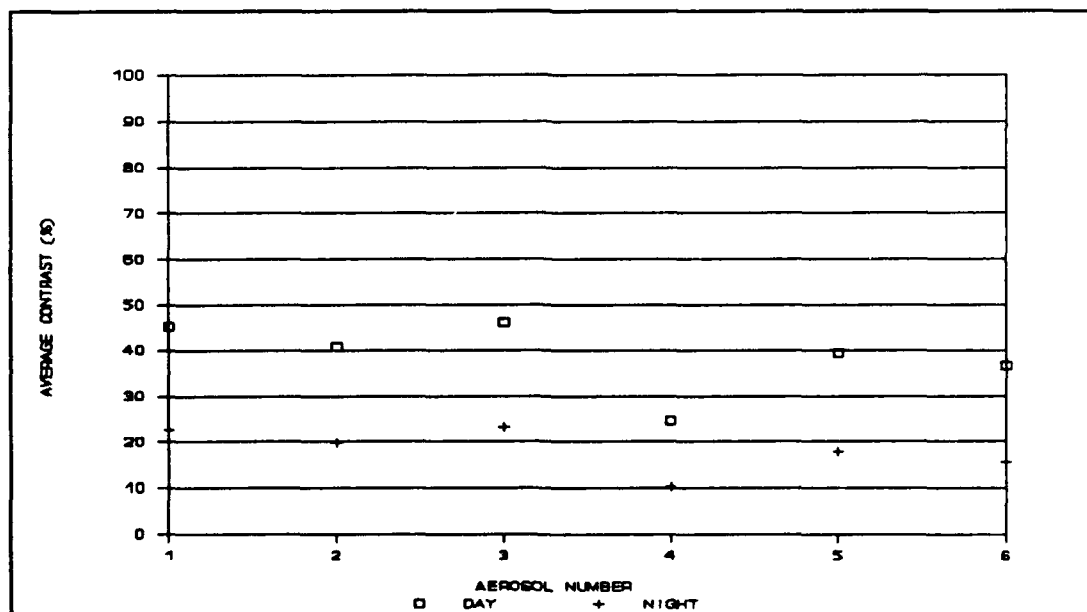
of it in the air as the wind speed increases, as is clearly seen in the results). The following is a discussion of what happens to the contrast when different boundary layer aerosols are present. The choices tested are shown in Table 4.

Table 4  
Boundary Layer Aerosols Tested

<u>Number on Graphs</u>	<u>Aerosol Type</u>	<u>LOWTRAN7 Default VIS</u>	<u>LOWTRAN7 Inputs</u>
1.	rural	VIS=23km	IHAZE=1
2.	maritime	VIS=23km	IHAZE=4
3.	desert	VIS=65.806km	IHAZE=10, WSS=5m/s
4.	desert	VIS=16.346km	IHAZE=10, WSS=20m/s
5.	rural	VIS=5km	IHAZE=2
6.	urban	VIS=5km	IHAZE=5

VIS is meteorological range.

Shown in Figures 17, 18, and 19 are the average contrasts using InSb, PtSi, and HgCdTe detectors respectively.



**Figure 17** AVERAGE CONTRAST OVER THE 3.3-4.2 $\mu$ m BAND FOR EACH BOUNDARY LAYER AEROSOL (IHAZE), InSb DETECTOR, SCENARIO 2



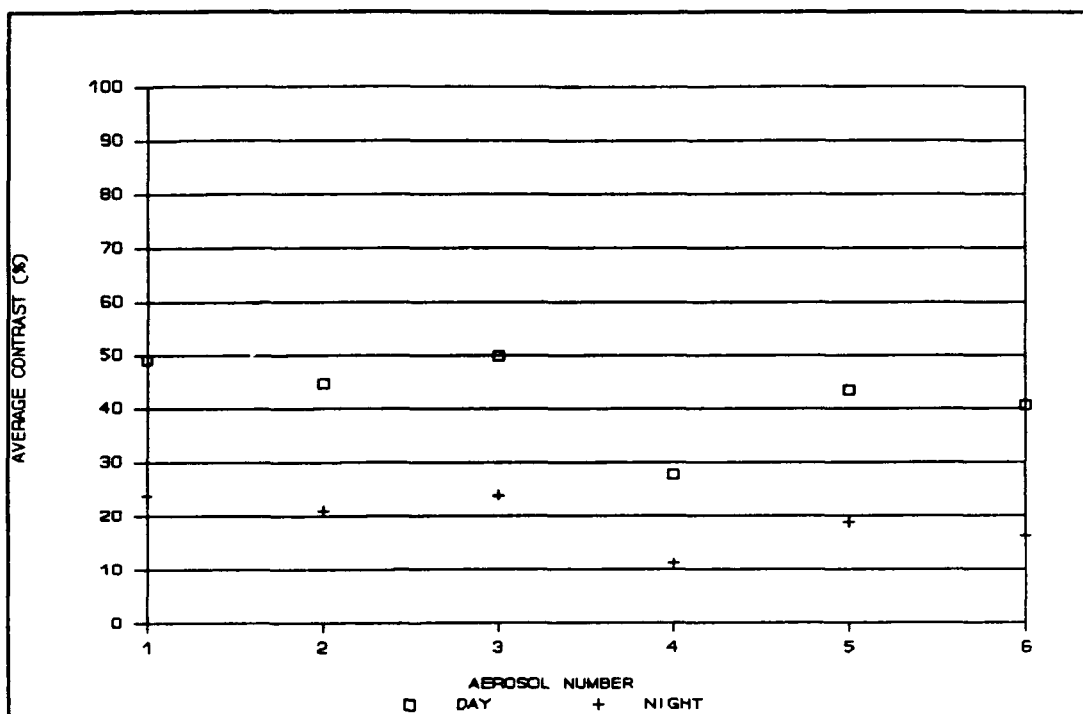


**Figure 18** AVERAGE CONTRAST OVER THE 3.3-4.2 $\mu$ m BAND FOR EACH BOUNDARY LAYER AEROSOL (IHAZE), Ptsi DETECTOR, SCENARIO 2

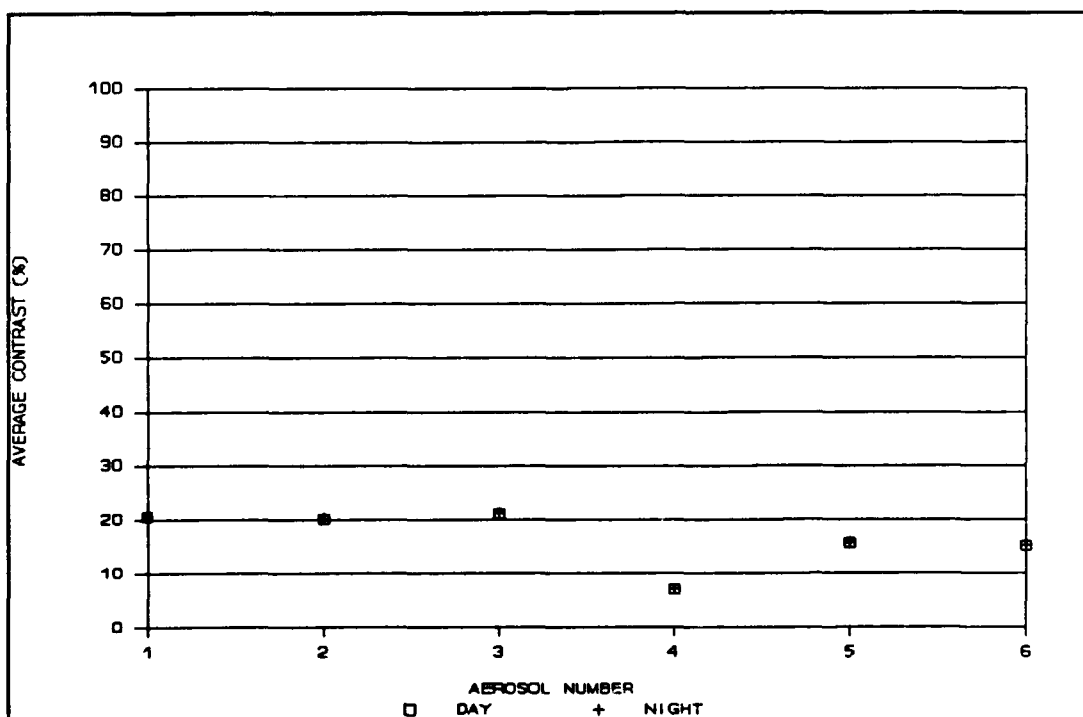


**Figure 19** AVERAGE CONTRAST OVER THE 8-12 $\mu$ m BAND FOR EACH BOUNDARY LAYER AEROSOL (IHAZE), HgCdTe DETECTOR, SCENARIO 2

The maximum difference between the contrasts in the 3.3-4.2 band is approximately 22%. Aerosols become an important factor in some cases. For example, if a system needs a 20% contrast to discriminate the target from the background, it would be useless in the presence of the last three aerosols. In the 8-12 band, all the contrasts are around 20% or less, rendering the system completely useless.

An important point demonstrated in these results is that the change in contrasts is not directly proportional to the change in VIS (meteorological range). This indicates the dependence of contrast on aerosol size and type. Again, these are difficult calculations easily performed with LOWTRAN7.

iv. Varying Atmospheric Profiles (MODEL).

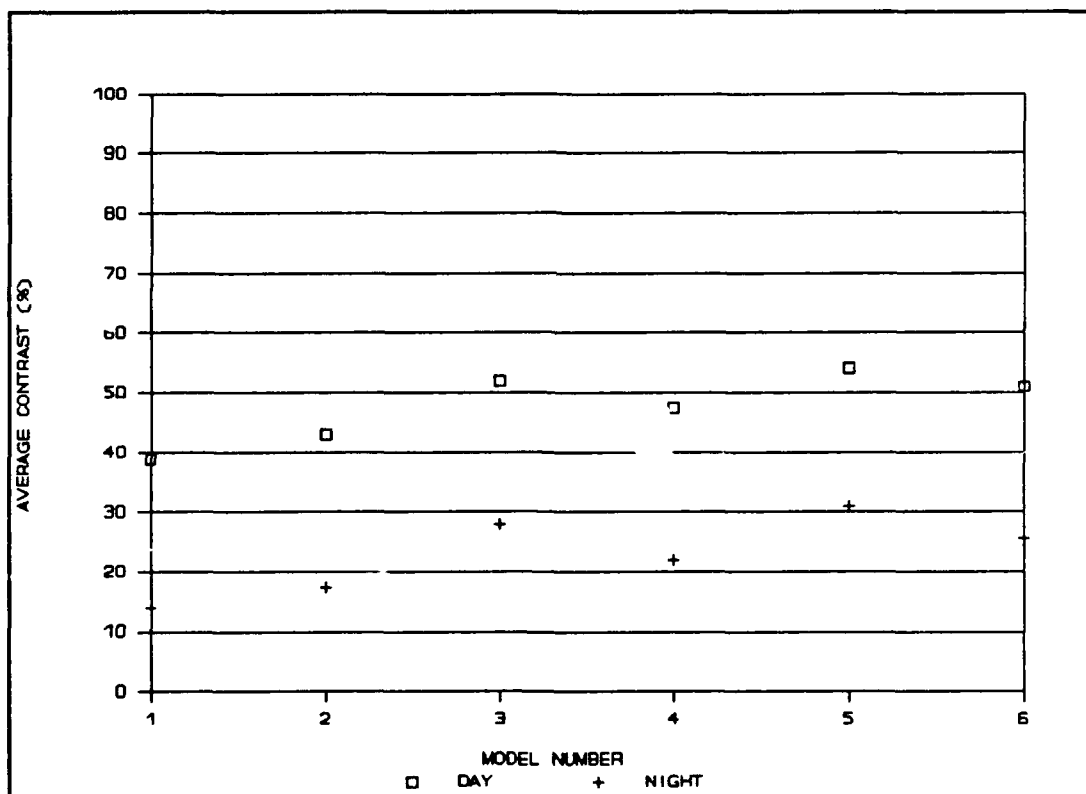
In the LOWTRAN7 program, there are six choices for atmospheric models. The following is a demonstration of the effect of changing the atmospheric model. The models tested are shown in Table 5.

Table 5  
Atmospheric Models Tested

<u>Number on Graph</u>	<u>Model Description</u>	<u>LOWTRAN7 Input</u>
1.	tropical	MODEL=1
2.	midlatitude summer	MODEL=2
3.	midlatitude winter	MODEL=3
4.	subarctic summer	MODEL=4
5.	subarctic winter	MODEL=5
6.	1976 U.S. standard atmosphere	MODEL=6

The type of model defines the atmospheric profile used in the calculations. For example, a subarctic climate has cooler temperatures and less water vapor than a tropical climate (12). The 'tropical' latitude is 15°N, the 'midlatitude' latitude is 45°N, and the 'subarctic' latitude is 60°N (12).

Figures 20 through 22 show the contrasts calculated.



**Figure 20** AVERAGE CONTRAST OVER THE 3.3-4.2 $\mu$ m BAND FOR EACH ATMOSPHERIC PROFILE (MODEL), InSb DETECTOR, SCENARIO 2

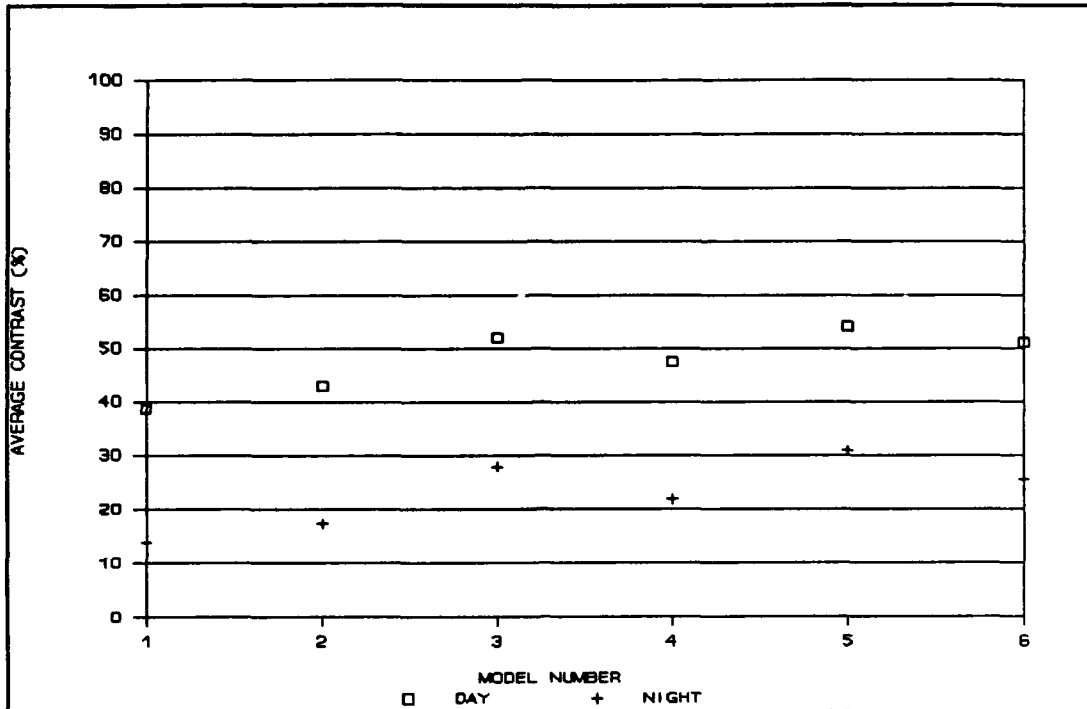


**Figure 21** AVERAGE CONTRAST OVER THE 3.3-4.2 $\mu$ m BAND FOR EACH ATMOSPHERIC PROFILE (MODEL), PtSi DETECTOR, SCENARIO 2

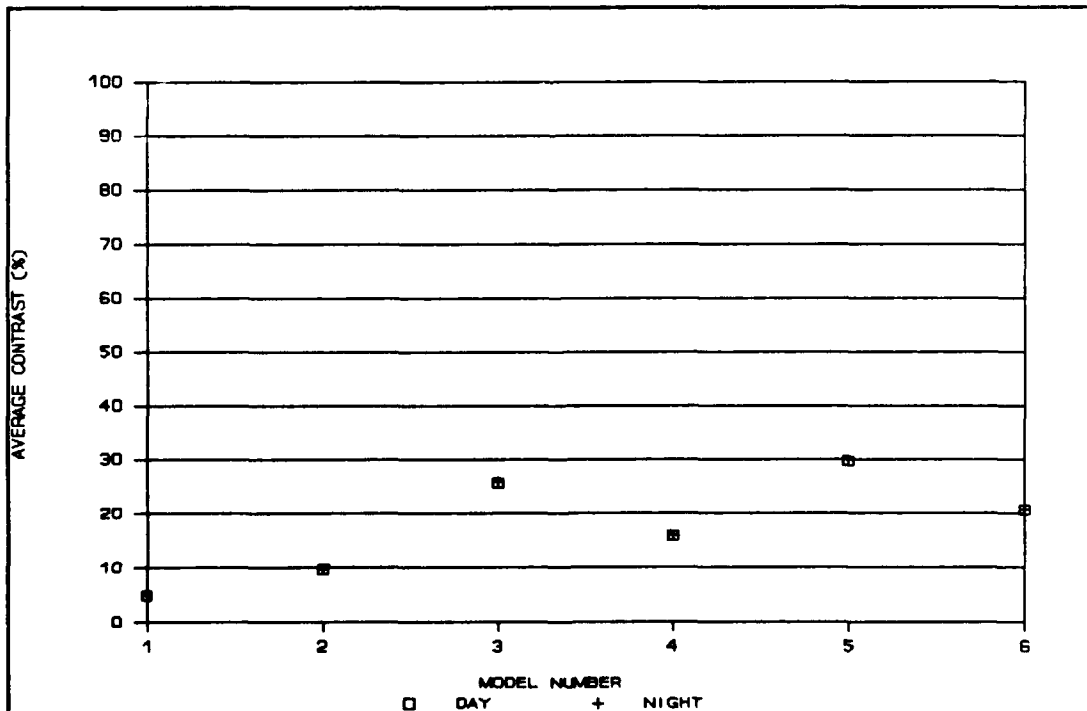


**Figure 22** AVERAGE CONTRAST OVER THE 8-12 $\mu$ m BAND FOR EACH ATMOSPHERIC PROFILE (MODEL), HgCdTe DETECTOR, SCENARIO 2

The largest difference in the contrasts are between the tropical model and the subarctic winter model. This is expected, since the tropical model and the subarctic winter model have the largest temperature (thus pressure, water vapor, and constituent profile) differences (12).

One interesting point is that in the 8-12 band, the contrast when using the tropical model drops more than in the 3.3-4.2 band. Since nothing about the target and the background changes, the decrease in contrast must be caused by a decrease in the transmittance. When the transmittance mode is run and the constituent transmittances are examined, it is seen that water vapor causes the transmittance to drop more in the 8-12 band than in the 3.3-4.2 band when going from the subarctic winter to the tropical model, because the water vapor continuum causes a very large decrease in the 8-12 band and a relatively small decrease in the 3.3-4.2 band. The tropics have higher humidities than other models, so the effect of water vapor and the stronger effect of the water vapor continuum in the 8-12 band is more noticeable (12).

v. Varying Relative Humidity.

LOWTRAN7 allows the user to input relative or absolute profiles. This subsection describes the effects of varying the relative humidity on the contrast detected.

Relative humidity is "the ratio of the actual vapor pressure of the air to the saturation vapor pressure at the ambient air temperature" (13). When the relative humidity

increases, and the air approaches saturation, the particles in the air actually grow because they begin to stick together. The growth is exponential with the increasing relative humidity. With relative humidities above 75%, the particles become large enough to have substantial scattering effects (14). Therefore, relative humidity is a primary factor in the amount of scattering that occurs (15).

Relative humidity is measured in percent and entered in the bottom 6 layers only in this test. The relative humidities above 6km are deferred to the 1976 U.S. Standard Atmosphere (MODEL=6). The values of relative humidity for each of the first six layers are increased from the standard atmosphere model value by a constant percentage for each run. The percentages of increase are: 10%, 20%, 30%, 40%, and 48%.

The results for this test are shown in Table C1 in Appendix C. As expected, the contrast decreases as the relative humidity increases. This effect is more apparent in the 8-12 band as the water vapor continuum is again the dominant factor. In the 3.3-4.2 band, the drop is approximately 3% from the two outer points. In the 8-12 band, the same drop is approximately 8%. In all of the 8-12 band cases, the contrast detected is below 20%. Using the LOWTRAN7 program, it is fairly easy to input any relative humidity profile to calculate its influence on transmittance.

vi. Varying Absolute Humidity.

Absolute humidity is "the mass of water vapor in a unit volume of air" (13). The units used in this test are grams/meter<sup>3</sup>. When looking across the desert, the air may look very clear, and the relative humidity may be fairly low. If the temperature is high, however, the air can hold a lot more water vapor (therefore having a higher absolute humidity) and this can reduce the transmittance significantly. In this manner, changing absolute humidity primarily affects molecular absorption (13).

Absolute humidity profiles can also be modified using the LOWTRAN7 program. In this study, the absolute humidity is increased from the standard atmospheric model value by a constant percentage for each run for the first 6km of the atmosphere. Its value above 6km is deferred to that of the 1976 U.S. Standard Atmosphere. The percentages of increase are: 10%, 20%, 30%, 40%, and 50%.

The program calculates a relative humidity for each atmospheric layer based on the absolute humidity and the temperature of that layer. The relative humidities calculated are lower than those tested in the previous section. Changing the absolute humidity by the above percentages only changes the relative humidity by a few percent.

The results of this section are shown in Table C2 in Appendix C. As in the relative humidity tests, the contrast decreases as the absolute humidity increases, and the 8-12

band is affected more than the 3-5 band due to the water vapor continuum.

The changes when varying the absolute humidity are slightly greater than the changes when varying the relative humidity which is consistent with a result previously reported by Condray (16). This indicates that varying absolute humidity (thus the amount of molecular absorption) has more affect on the amount of radiation transmitted at these wavelengths than varying relative humidity (thus the amount of scattering). This is expected, since scattering has more affect on the wavelengths from the visible to the near IR ( $\sim 0.4\mu\text{m}$  to  $3\mu\text{m}$ ) than in the longer wavelength region used in this study.

vii. InSb vs. PtSi.

LOWTRAN7 helps make comparisons between different detector materials. The difference between InSb and PtSi, based on the assumptions used in this study, is their quantum efficiencies (see Table 1). The responsivity of PtSi is plotted in Figure 12 on page 37. InSb responsivity, given by Equation 8, is plotted in Figure 23. Since thermal contributions are increasing across the 3-5 band, and the responsivity of InSb is increasing, as opposed to that of PtSi, InSb should be affected more by thermal contributions than PtSi. Conversely, solar contributions are decreasing across the 3-5 band, so PtSi should be more sensitive to solar radiation.



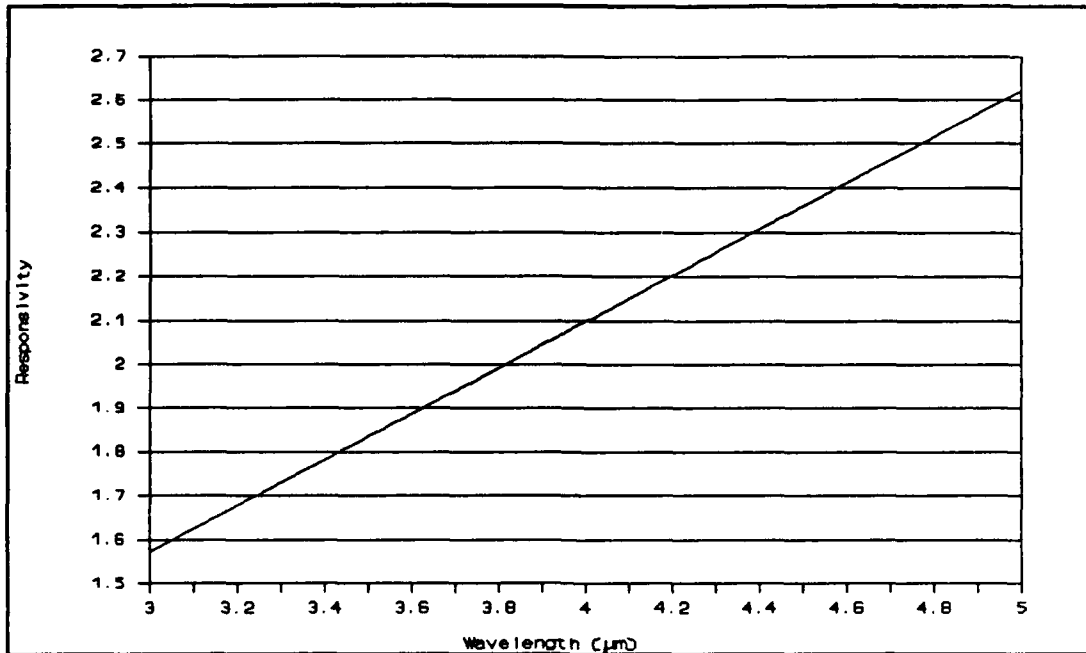


Figure 23 InSb RESPONSIVITY VS. WAVELENGTH

LOWTRAN7 results used in the contrast equation demonstrate quantitatively the effect of each material's different sensitivity in different situations. During the daytime scenarios, the contrast using PtSi is approximately 5% higher than that when using InSb. At night the two detectors give about the same contrast, and since no thermal variations are tested, the InSb is not expected to change. These results are compatible with the expectations.

## V. System 2: A Non-Imaging System

This chapter discusses the results when the CS is calculated using a non-imaging system.

When CS is calculated for scenario 1, the values are negligible. The reason that the CS is so small, even when contrasts may be as much as 50%, is because of the basic assumptions made when defining the imaging and non-imaging systems. In the imaging system, the target is large compared to the instantaneous field-of-view. The input signal across each of the entire fields-of-view compared is different. In the non-imaging system, the target is small with respect to a single detector's field-of-view. Only a small fraction (1%) of the input signal of the field-of-view changes. The difference that the change in the small fraction makes is negligible when the target and background are so similar (as in scenario 1).

Scenario 2 is used to show that under more realistic conditions, a CS can be measured. In scenario 2, the range is shortened from 23km to 18km, so that the footprint of the sensor is smaller and the target area is more realistic (the target area is still assumed to be 1% of the footprint area). A vertical sky-to-ground path is used, and the target temperature is increased to 400°K.

These results demonstrate the difference that changing one scenario parameter (target temperature) and the figure-of-

merit measurement can make. For the CS evaluation, the baseline test is run using the rural aerosol with a 23km meteorological range and a vegetation background. The next test is changing the background to snow. The next six tests are the CS calculated from the two boundary layer aerosols with the largest difference in contrast, the two atmospheric models with the largest contrast difference, and the two relative humidities with the largest difference in contrast. The results are shown in Table 6.

Table 6  
Average CS Calculated Using Different Variables in  
Scenario 2, in the 3.3-4.2 and 8-12 $\mu$ m Wavebands

Variable	InSb Day 3.3-4.2 $\mu$ m	InSb Night 3.3-4.2 $\mu$ m	PtSi Day 3.3-4.2 $\mu$ m	PtSi Night 3.3-4.2 $\mu$ m	HgCdTe Day 8- 12 $\mu$ m
Baseline	9.20	16.57	9.09	17.52	1.34
Snow Back- ground	13.22	15.18	13.75	16.15	1.27
Desert, WSS=5m/s	9.82	16.66	9.84	17.60	1.36
Desert, WSS= 20m/s	7.68	13.94	7.59	14.78	1.04
MODEL= tropical	8.41	13.79	8.30	14.33	.89
MODEL= subarct. winter	9.90	18.05	9.75	19.13	1.51
Rel Hum Increase 10%	9.32	16.75	9.25	17.73	1.33
Rel Hum Increase 48%	8.73	16.21	8.62	17.07	1.17

i. General Results.

In scenario 1 the target and background temperatures are the same, but in the current scenario they are approximately 100°K different. Changing the temperature causes significant differences in these results as compared with those in the previous chapter, but by using the LOWTRAN7 program to do the calculations, the effects are easily evaluated. The temperature difference means a difference between the target and background thermal radiances. As a result, two significant differences from contrast results are seen.

The first noticeable difference is that the CS in the 8-12 $\mu$ m band is very small compared to the CS in the 3.3-4.2 band. To explain this result, the blackbody curves for the target and background radiances multiplied by their respective emissivities are plotted in Figure 24.

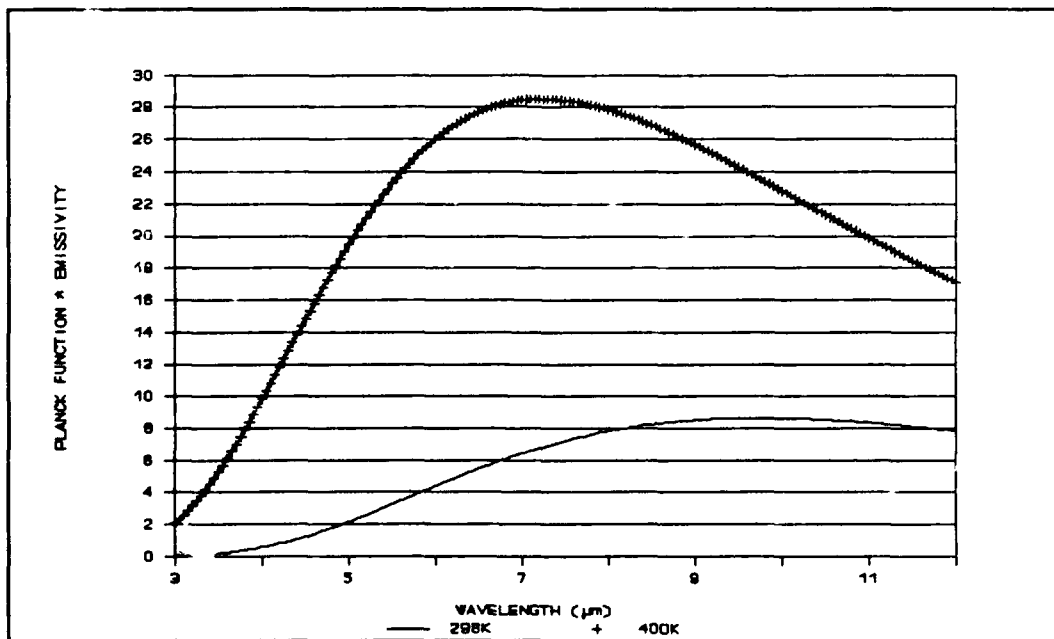


Figure 24 BLACKBODY RADIANCE TIMES EMISSIVITY VS. WAVELENGTH

The higher temperature of the target, in spite of its lower  $\epsilon$ , causes its curve to be much larger than that of the background. The actual difference between the target and background is higher in the 8-12 band, but since both signals are smaller in the 3.3-4.2 band, the percent difference is greater. Thus, a larger CS is measured in the 3.3-4.2 band.

The second difference is that the nighttime CS values are much higher than those in the daytime in the 3.3-4.2 band, as opposed to the results of the previous section. In the daytime scenario, total radiance is increased by the addition of solar radiation, so that, even though the target signal increases slightly more because of its higher reflectivity, the fraction of change is smaller. Thus CS calculated is less than in the daytime.

ii. Varying Background.

Changing the background from vegetation to snow yields different results from those in Chapter 4. These results are difficult to predict or explain, but by examining the output of the program, they are fairly easily understood. Table 7 shows only the effective radiance values from LOWTRAN7 at one wavelength, but the reasons for the CS values calculated can be understood by examining their relative sizes.

Table 7

Effective Radiances for Vegetation and Snow Backgrounds  
at 4 $\mu$ m Obtained from LOWTRAN7

Effective Radiance (W/cm <sup>2</sup> -sr- $\mu$ m)	Vegetation Background	Snow Background
Target Thermal	.000824	.000824
Background Thermal	.000051	.000055
Target Reflected	.000069	.000069
Background Reflected	.000019	.000004
Target Total	.000893	.000893
Background Total	.000070	.000059

The target thermal radiance is completely dominant over any other radiance. As background emissivity is increased (from vegetation to snow), its thermal radiance increases very slightly. So the nighttime CS decreases as the target and background radiances become closer together. In the day scenario, as background emissivity decreases (from vegetation to snow), its reflected radiance decreases more than its thermal radiance increases, decreasing the total background radiance. This makes the difference between the target and background radiances greater. Thus, when using a background with a higher emissivity, the daytime CS is greater. The difference between the day and night values of the CS is explained in section i., using the blackbody curves.

iii. Varying Boundary Layer Aerosols (IHAZE),  
Atmospheric Models (MODEL), and Relative  
Humidity.

Changing the boundary layer aerosol, the atmospheric profile, and the relative humidity have the same effects on CS calculations as they do on contrast calculations, but to different degrees because of the different scenario, as shown in the data tables. LOWTRAN7 is useful in determining the quantity of change for any given situational change.

iv. InSb vs. PtSi.

The additional effect of solar contributions in calculating the CS, as discussed above, is to degrade the CS. When PtSi is used, there is more degradation in the CS, which is expected since the PtSi depends more on solar effects than the InSb. The InSb shows a slightly lower CS than the PtSi at night. This is probably because the background emissivity is higher, making its thermal radiance closer to that of the target, thus reducing the CS, illustrating that the InSb is more sensitive to thermal effects. Again, LOWTRAN7 is very useful in analyzing the effectiveness of different detector materials in different situations.

## VI. Single and Multiple Scattering

The effect of multiple scattering on figures-of-merit is extremely difficult to predict. This chapter describes some trends found in this project. The primary purposes of this chapter are to demonstrate the necessity, when using LOWTRAN7, of considering multiple scattering effects, and to demonstrate how useful it is in analyzing this difficult problem.

### SALB

One factor that affects multiple scattering is the SALB (average boundary reflectivity). The SCR, calculated at one wavelength where the contrast corresponds to the average contrast across the band (3.3-4.2 and 8-12 $\mu\text{m}$ ) is plotted as a function of SALB for the daytime InSb case in Figure 25. Plots for the night InSb, day PtSi, night PtSi, and day HgCdTe cases are shown in Appendix C, Figures C12 through C15.

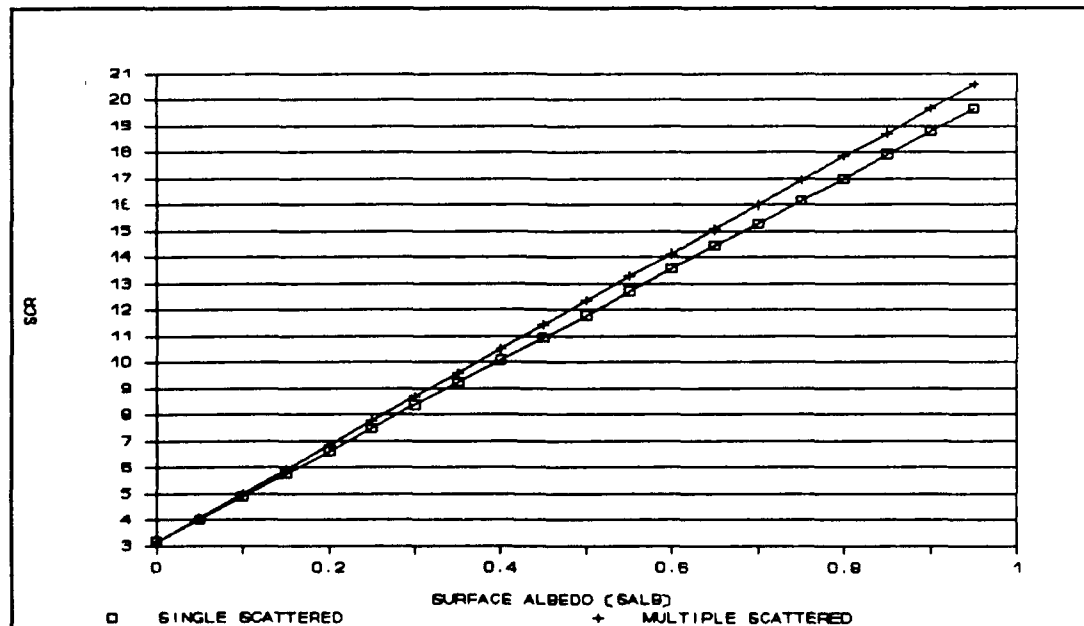


Figure 25 SCR EVALUATED AT 3.802 $\mu\text{m}$ , InSb DETECTOR, DAY



(In these tests, a ground-to-space vertical geometry is used with the baseline parameters). Several trends are present in the results. First of all, the multiple scattering adds more to the SCR as the SALB increases. When the SALB is higher, more solar radiation is reflected and multiple scattered. Secondly, the multiple scattering effect is greater in the 8-12 band than in the 3.3-4.2 band. Another effect is that multiple scattering adds a larger absolute amount of input radiance in the daytime case, as is expected since solar radiation adds to the amount of radiation that can be multiple scattered.

A fourth effect is that the addition of multiple scattered radiance causes the radiance value to increase. Single scattering predicts radiation being scattered into the path, whereas multiple scattering predicts radiation being scattered into and out of the path (7). One would expect, therefore, that the multiple scattered value would be lower. Initial validation tests run by the LOWTRAN7 experts at the Geophysics Laboratory used a geometry opposite of that used in the present work - looking from the ground to the sky. In cases tested there, the multiple scattering radiance was actually lower than the radiance calculated without it (7). The program authors assumed that different geometries would not change the fact that the radiance decreases with the addition of multiple scattering; however, the trials presented in this chapter, as validated by Geophysics Laboratory on 26

September, show that multiple scattering causes an increase in the radiance. This effect is as yet unexplained. Concentrations of scatterers at different points in the path cause different effects, so the situation is much more complex than it appears at first glance. This contradiction demonstrates the difficulty in predicting the effect of multiple scattering.

Another point to be noted is that because of the dependence of multiple scattering on SALB, if the target and background reflectivities are different, multiple scattering affects them differently.

#### Aerosols

A second parameter that affects multiple scattering is the atmospheric density. The effect of increasing the atmospheric aerosol density and using multiple scattering versus single scattering is demonstrated in the following comparisons. The rural, 23km VIS aerosol, (baseline) and the high wind desert aerosols are compared. The contrast using scenario 1 is calculated and the CS using scenario 2 is calculated. The results are given in Tables 8 and 9.

**Table 8**

**Multiple Scattering Effects on Contrast Calculations**  
**Using Scenario 1**

Variable	InSb Day (3.3- 4.2 $\mu$ m)	InSb Night (3.3- 4.2 $\mu$ m)	PtSi Day (3.3- 4.2 $\mu$ m)	PtSi Night (3.3- 4.2 $\mu$ m)	HgCdTe Day (8- 12 $\mu$ m)
Baseline/ Single Scattered	44.22	25.00	50.98	25.58	21.63
Baseline/ Multiple Scattered	46.34	20.19	50.05	21.05	16.35
Desert, Wind Speed = 20m/s Single Scattered	24.49	10.47	27.70	11.12	7.15
Desert, Wind Speed = 20m/s Multiple Scattered	40.36	16.67	43.08	17.20	10.39

Table 9  
Multiple Scattering Effects on CS Calculations  
Using Scenario 2

Variable	InSb Day (3.3- 4.2 $\mu$ m)	InSb Night (3.3- 4.2 $\mu$ m)	PtSi Day (3.3- 4.2 $\mu$ m)	PtSi Night (3.3- 4.2 $\mu$ m)	HgCdTe Day (8- 12 $\mu$ m)
Baseline/ Single Scattered	9.20	16.57	9.09	17.52	1.34
Baseline/ Multiple Scattered	10.02	16.33	10.09	17.28	1.38
Desert, Wind Speed = 20m/s Single Scattered	7.68	13.94	7.58	14.78	1.04
Desert, Wind Speed = 20m/s Multiple Scattered	25.30	13.48	27.05	14.31	1.04

The results in Tables 8 and 9 demonstrate the variety of effects caused by adding multiple scattering to the calculations. Among the differences, there are several trends shown in the above results. One is that the high aerosol scenario (desert) is affected much more than the low atmospheric density scenario (rural), which is expected. The other effect is that when the density is higher, the contrasts and the CS are improved. The reason for the second effect is that under windy desert conditions, the transmittance is decreased. The transmitted radiance is decreased, so the output signal of the detector is

decreased. The percent difference between the target and the background signals is therefore greater, increasing the contrast or CS. This is a case where, even though the figures-of-merit used in this study indicate good results, it is important to evaluate other figures-of-merit that consider the size of the input signal necessary for discrimination. Day and night scenarios are influenced differently under different conditions. Multiple scattering also affects the 3-5 and 8-12 wavebands differently. The LOWTRAN7 program is extremely useful in handling the complicated analysis of multiple scattering.

## VII. Conclusions and Recommendations

The LOWTRAN7 computer model provides useful information for electro-optic system design and analysis. In this project, the atmospheric transmittance and radiance information provided by LOWTRAN7 is used to estimate electro-optic system performance using hypothetical figures-of-merit. The methods used in the analysis are described, and general trends are found and identified to illustrate the type of information this analysis provides.

In the generic imaging system, the figure-of-merit used is contrast. Using LOWTRAN7 radiance and transmittance outputs and the quantum efficiency of the detector material, the SCR can be calculated for one detector that sees only the target and an adjacent detector that sees only the background. The contrast, which is the average difference between the two signals divided by the target signal, is calculated. For contrast evaluation neither specific system information nor the actual current output of the detector needs to be known.

Many of the conditions that affect the SCR, thus affecting the contrast can be varied in LOWTRAN7, such as: background emissivity; boundary layer aerosols; atmospheric profiles; relative humidity; and absolute humidity. This paper describes what information can be determined from LOWTRAN7 by changing the previously mentioned conditions.

The characteristics of a background that affect the amount of contrast are its temperature and its emissivity. When target and background temperatures are the same, the larger the difference between their emissivities, the larger the contrast.

Another factor that affects the amount of contrast is the type of boundary layer aerosol. Contrast change is not directly proportional to the change in meteorological range, because it depends on the size and type of aerosols present, and the waveband of interest.

Varying the atmospheric profile (with the MODEL input) also changes the amount of contrast. This change depends heavily on humidity: in the subarctic winter where the humidity is the lowest, the contrast is the highest; in the tropical model where the humidity is highest, the contrast is lowest. This could be a very important consideration when designing an electro-optic system to be used in tropical latitudes - the system's efficiency, especially in the 8-12 band (as the water vapor continuum has a significant effect in this range) could be less than its efficiency under standard atmospheric conditions.

Increasing relative humidity increases the scattering effect, thus decreasing contrast slightly. It affects the 8-12 band more than the 3-5, again because of the absorption in the 8-12 band by the water vapor continuum.

Increasing absolute humidity increases molecular absorption, especially in the 8-12 band, thereby reducing the contrast.

The greater sensitivity of PtSi to solar reflected radiation causes it to show approximately 5% more contrast than the InSb detector in the daytime. At night, both detectors show approximately the same contrast. The LOWTRAN7 calculations of the relative thermal and reflected radiance sources help to demonstrate the different detectors' strengths under different conditions.

In the non-imaging system a useful figure-of-merit is the change in signal (CS), which is the difference between the signal with and without the target divided by the signal without the target. Since a basic assumption of the second system is that the target is very small compared to the footprint area (as opposed to system 1), there is a dependence on range (not seen in system 1). An assumption made in this study is that the target and background lie in the same plane, which is fixed. Under this assumption, only the ratio of the target area to the footprint area needs to be known. If the target is assumed to be completely in or completely out of the field-of-view, and the ratio of the target area to the footprint is known, Equation 19 is used to calculate the CS.

When the CS is calculated in scenario 1 above, with the target approximately 1% of the footprint area, there is basically no CS. The reason that system 2 will see no



discernable change in signal, even when system 1 will see a 30-40% contrast, is due to the primary assumption made about each system. In the imaging system (system 1), it is assumed that the target is large relative to the footprint of the detector. A contrast is made between the output signals produced by one footprint filled with background and one footprint filled with target. In the non-imaging system (system 2) it is assumed that the target is small relative to the footprint. A comparison is made between the output signals due to one footprint filled with background and one footprint filled with background except for 1%, and that 1% has the target signal. In the non-imaging system, therefore, changing the already small target radiance by a small amount produces little change in the whole input signal, resulting in little change in the output signal of the detector.

When scenario 2 is tested, with a 400°K target at 18km that has an area 1% of the footprint area, there is a detectable signal change in the 3.3-4.2 band, but only a very small change in the 8-12 band. (The 3.3-4.2 band is used throughout this study because it shows the best contrast and the most transmittance.) In the 3.3-4.2 band, the daytime CS for the conditions tested is about half the nighttime CS (unlike the results from system 1). This is due to the fact that even though there is more actual change in the signal during the day, the solar contribution to the input signal is much larger. The percent change is, therefore, quite a bit

smaller. In the cases tested, it would be easiest to see the target in the 3.3-4.2 $\mu$ m band at night. These results demonstrate how changing one parameter or the figure-of-merit definition can significantly alter the results. It also demonstrates the usefulness of LOWTRAN7 in adapting to different situations.

Changing atmospheric conditions, as in system 1, produces the same general trends. Varying boundary layer aerosols varies the CS. Using atmospheric models with higher humidities decreases the CS. Increasing the humidity decreases CS. The only difference from the contrast trends is the different background emissivity (snow vs. vegetation). When the temperature difference, the emissivity difference, and the reflectivity difference are all considered in the waveband of interest, the snow-background CS is larger than the vegetation-background CS during the day but smaller than the vegetation-background CS at night. This result would be difficult to predict, but the program is extremely useful in determining it.

The CS may be a positive or a negative number. According to Equation 19, it is positive (the signal increases when the target enters the field-of-view), if the target signal is higher than the background signal; and vice versa. In scenario 2, the target thermal radiance is higher because the target is hotter, and the target reflected radiance is higher, so the CS is positive in all cases tested.

Multiple scattering effects (which are not generally considered in this analysis) may degrade or improve the contrast or the CS. Multiple scattering has a greater effect when the atmospheric density is higher (i.e., in the presence of greater relative humidity or more aerosols) and when the SALB input is higher (because there is more reflected radiance to multiple scatter). These effects are difficult to predict, and should always be used or checked for any type of LOWTRAN7 radiance use.

In summary, there are many atmospheric, target, and background characteristics that affect a detection system's performance, and LOWTRAN7 is extremely useful in evaluating these effects.

#### Suggestions/Recommendations

For further investigations of using LOWTRAN7 to evaluate detection systems, it may be interesting to study several things.

A good way to check the accuracy of the program for the purposes presented in this paper would be to compare LOWTRAN7 predicted results with results using real scenario parameters and a specific system. Another interesting topic is noise. Noise may come from the detection system or from the scenario. No matter what the contrast or the CS is, if the noise is too high, the target cannot be discriminated. Noise is a critical factor to consider when evaluating a detection system, and a

noise analysis could be performed in the form of an appropriate figure-of-merit.

As shown in Chapter 6, multiple scattering has very unpredictable effects, and should always be checked when using LOWTRAN7. An evaluation of trends of the multiple scattering effects as predicted by LOWTRAN7 in various situations, including with different viewing directions, would be an extremely interesting and useful study.

Three recommendations about the program are suggested by this study. One is that a common PC version for all users would be beneficial. With different programs and different sets of errata, comparisons are more difficult to make. The common version could have separate output files, one in  $\mu\text{m}$  and one in  $\text{cm}^{-1}$ , that are in ascii format for easy importation into other programs. Another suggestion is that some way to input a variable reflectivity be devised. Even averages made for the snow and vegetation used in this project vary quite a bit (9). A third suggestion is that a comprehensive updated LOWTRAN7 manual be written, containing sections of detailed calculations, sections of general explanation, and quirks in running the program.

## Appendix A: Input Parameters

The basic instructions for how to run LOWTRAN7, such as specifically what inputs are necessary, are outlined in the LOWTRAN7 Technical Report (6). The purpose of this appendix is to step through the input parameters, show how they were input for this study, and make some points, or in some cases, reemphasize points in the instructions in the LOWTRAN7 Technical Report about the inputs used in this project (6). The input section is divided into five "cards" and several subcards that may or may not be used depending on what the primary inputs are.

### Card 1

The first parameter in Card 1 is MODEL. This determines what atmospheric model is used in the calculations. In this scenario, the 1976 U. S. Standard Atmosphere, MODEL=6, is chosen for all baseline tests.

The next input is the type of path, ITYPE. The choices are: 1) horizontal (constant-pressure) path, 2) vertical or slant path between two altitudes, or 3) vertical or slant path to space. For the first scenario studied, the sensor is looking from space to earth, thus ITYPE=2 is chosen. It happens that ITYPE=3 gives the same geometrical results for scenario 1. If the user is not sure which ITYPE to use, he can pick one and check the geometry calculations in the output file to ensure the program is doing what is intended. This is

very important in some scenarios, particularly since there are several ways to input the geometric parameters, as described later.

The next input, IEMSCT, determines what the program will calculate. For each "mode" there are several outputs:

IEMSCT=0: Transmittance mode - frequency ( $\text{cm}^{-1}$ ), wavelength ( $\mu\text{m}$ ), total transmittance,  $\text{H}_2\text{O}$  transmittance,  $\text{CO}_2$  transmittance, ozone transmittance, trace transmittance,  $\text{N}_2$  continuum transmittance,  $\text{H}_2\text{O}$  continuum transmittance, molecular scattering transmittance, aerosol-hydrometeor (aer-hyd) transmittance,  $\text{HNO}_3$  transmittance, and integrated absorption.

IEMSCT=1: Thermal radiance mode - frequency, wavelength, atmospheric radiance ( $\text{cm}^{-1}$  and  $\mu\text{m}$ ), integrated radiance, and total transmittance.

IEMSCT=2: Radiance mode with solar/lunar single scattered radiance - frequency, wavelength, atmospheric radiance ( $\text{cm}^{-1}$  and  $\mu\text{m}$ ), path scattered radiance ( $\text{cm}^{-1}$  and  $\mu\text{m}$ ), ground reflected radiance ( $\text{cm}^{-1}$  and  $\mu\text{m}$ ), total radiance ( $\text{cm}^{-1}$  and  $\mu\text{m}$ ), integrated radiance ( $\text{cm}^{-1}$ ), and total transmittance.

IEMSCT=3: Directly transmitted solar irradiance - frequency wavelength, transmitted solar irradiance ( $\text{cm}^{-1}$  and  $\mu\text{m}$ ), incident solar irradiance ( $\text{cm}^{-1}$  and  $\mu\text{m}$ ), and integrated incident and integrated transmitted solar irradiances ( $\text{cm}^{-1}$ ), and the total transmittance.

Each mode gives an average transmittance; where applicable, maximum and minimum radiances are also reported. (A much more thorough explanation of the transmittance and radiance is given in Chapter 2). For this scenario, IEMSCT=2 is used.

The next choice, IMULT, decides whether to use single or multiple scattering. (This is obviously only used when IEMSCT=1 or 2). Multiple scattering, as discussed in the background, is important when the particle density of the atmosphere is high or when clouds are present. When the SALB is higher, multiple scattering is more important because there is more reflected radiance to scatter. The multiple scattering mode takes much longer to run than the single scattering mode, so it is not used in this study (though several runs are made to determine how much it does affect the output, and specific cases where it becomes important are discussed). IMULT=0 is generally used.

The next parameters, M1 through M6, and MDEF, are used to supplement various profiles, but when the U. S. Standard Atmosphere is chosen, they default to the model number (6 in this case), and the U. S. Standard profiles are input by the program. The next parameter, IM, defaults to 0 when an atmospheric model is chosen; it just has to do with the user-input profiles. When varying the relative and absolute humidity profiles (other parameters may be changed as well), however, MODEL=7 is chosen. In this case, the user is prompted to input the pressure, temperature, water vapor,

ozone, nitrous oxide, methane, and carbon monoxide amounts for each of the number of atmospheric layers, which the user also specifies. The user has a choice of several units for these profiles. If the user wants to apply a user-defined profile for several consecutive runs, on the second time through the card generation he should choose MODEL=7 again and set IM=0; the program will then refer to the previously input profile again without it actually being input again.

The next parameter, NOPRT, lets the user choose whether or not to have all the atmospheric profiles in the output file. These profiles take an enormous amount of paper and computer space, and are not necessary for this study, so NOPRT=1 is used.

The next two choices, TBOUND (boundary temperature - the boundary is what is at the end of the path such as an atmospheric layer, a cloud, or a target) and SALB (surface albedo), are given only in the radiance modes (IEMSCT=1 or 2). The boundary temperature ( $^{\circ}\text{K}$ ) can be set to something that the path intersects, such as a cloud or a target. If 0 is input for TBOUND, the program defaults TBOUND to the temperature of the atmospheric layer at the end of the path. At times, if the path does not intersect a particular object, the program will allow TBOUND =  $0^{\circ}$  without defaulting it. If one wants to make TBOUND =  $0^{\circ}\text{K}$ , (to get rid of the target thermal radiance and have the program calculate only path thermal radiance



discussed in the outputs-radiance section), TBOUND must be set to 0.01. Several TBOUNDS are used in this study.

Surface Albedo is the reflection of the boundary, and ranges from 0 to 1. (The definitions of albedo and reflectivity are discussed in Chapter 2.) The input SALB is the average reflectivity over the specified waveband of whatever is at the end of the path - target, vegetation, water, etc. Emissivity is not input, but calculated as  $1 - \text{SALB}$  by LOWTRAN7. If  $\text{SALB} = 0$ , then the surface is a blackbody, and emissivity = 1. As a reference, the average surface albedo of the earth ranges from about 0.3 to 0.5 (17). Reflectivities for various surfaces such as snow, grass, and coatings, are wavelength-dependent and may vary greatly; averages can therefore be extremely rough estimates. For this study the target reflectivity is assumed to be a constant 0.32 across both wavebands (not very realistic). The vegetation background has a variable reflectivity, so it is input as follows. The wavebands are broken up into subbands  $5\mu\text{m}$  across (which is chosen because the numbers on the graphs used are most easily read in increments of  $5\mu\text{m}$ ), an average reflectivity is assigned to each band, and each one is made a separate run of LOWTRAN. Although this is a time-consuming way to run the scenario, it is the only way to use a variable reflectively in the program at this time.

## Card 2

The first input in card 2 is IHAZE. This specifies the aerosols in the boundary layer (0 to 2km). The choice made also specifies a meteorological range (called VIS in the program). One distinction that should be noted is the difference between meteorological range and visibility. (Since VIS stands for meteorological range, not visibility). The correct mathematical expression for meteorological range is

$$VIS = \left( \frac{1}{\sigma} \right) \left( \ln \frac{1}{\epsilon} \right) \quad \text{Eq (25)}$$

where  $\sigma$  is an extinction coefficient and  $\epsilon$  is the threshold contrast (16). Visibility is defined as "the greatest distance at which it is just possible to see and identify with the unaided eye: (a) in the daytime, a dark object against the horizon sky; and (b) at night, a known moderate intensity light source" (6). If the user knows only the visibility, he can convert it to meteorological range using Equation 26 (6):

$$VIS = \text{visibility} * (1.3 \pm 0.3) \quad \text{Eq (26)}$$

The choices for IHAZE are as follows:

0=no aerosol extinction

1=rural extinction, VIS=23 km

2=rural extinction, VIS=5 km

3=Navy Maritime extinction (VIS depends on input  
wind and relative humidity that will

consequently be prompted)

4=maritime extinction, VIS=23 km

5=urban extinction, VIS=5 km

6=tropospheric extinction, VIS=50 km

7=user defined extinction - triggers subsequent  
cards

8=fog1 (advective) extinction. VIS=0.2 km

9=fog2 (radiative) extinction, VIS=0.5 km

10=desert extinction (VIS is calculated from the  
wind speed, WSS, input).

For the baseline scenario, IHAZE=1 is selected.

The next input parameter, ISEASN, determines the seasonal aerosol profile for tropospheric and stratospheric aerosols (2-10km and 10-30km, respectively) (6). The choices are:

0=defaults to the model

MODEL=0,1,2,4,6,7 gives spring-summer

MODEL=3,5 gives winter

1=spring-summer

2=fall-winter

ISEASN=0 is used in this study.

The next input is IVULCN, which determines the aerosol profile and the type of extinction for the stratosphere and above the stratosphere to 100km. The choices for IVULCN are shown on page 24 of the LOWTRAN7 Technical Report (6). IVULCN=0 is chosen for this scenario.

ICSTL is the next input parameter, which is only used with the Navy Maritime model. It describes the air mass character from the open ocean (ICSTL=1) to strong continental influence (ICSTL=10).

The next input is ICLD. This parameter gives the user a choice of no clouds, clouds, cloud models, or clouds with rain. The type of cloud, its base and top height, and the amount of rain for each choice are specified in the choices presented. If a cloud model is chosen, the user is prompted for more inputs to specify the cloud characteristics. ICLD=0 is used for this scenario, because any amount of clouds, rain, or fog makes the transmittance go to 0 in the case being studied.

The next input is VSA, or the Army Vertical Structure Algorithm, which describes aerosols in the boundary layer. This allows the user to input a more detailed profile in the bottom two kilometers of the atmosphere. This option is not used in the present study.

The next choice, VIS, allows the user to input some meteorological range other than that defined by the choice of IHAZE. If this is input as a non-zero number, then it will override the VIS in the IHAZE choice.

WSS, the current wind speed in m/s, is only necessary when the Navy maritime model or the desert model is chosen. When the desert is chosen in this study, WSS values used are 5 and 20 m/s. In the desert case, the VIS is calculated from

this input windspeed, as long as the VIS input is set to 0. If WSS=0 when the desert model is used, the default VIS (sea level meteorological range) is 75.711km. The higher the windspeed, obviously the lower the meteorological range.

WHH, the 24-hour average wind speed, is only used for the Navy maritime model, so it is not used in this test.

The next parameter is the rain rate, RAINRT, in mm/hr. When clouds are present (chosen in ICLD), the rain in the model decreases linearly to the cloud level. When no clouds are specified, the rain rate is constant up to 6km. This option is not used in the present study.

The final parameter on Card 2 is GNDALT. GNDALT selects the altitude above sea level of the ground. When the ground altitude is raised, the aerosol profiles of the lowest 6km of the atmosphere are compressed into the space between the ground altitude input and 6km above sea level (15). This may result in significant pressure differences.

Card 2 has several subcards, such as to specify cloud parameters when cloud models are chosen, or to specify more parameters for the Army Vertical Structure Model, but none of these are used in this study.

### Card 3

This card describes the geometry of the scenario. Several combinations of inputs can be used--it is not necessary to specify every parameter--and a good explanation

of which parameters to specify under which circumstances is given in the LOWTRAN7 Technical Report, page 36 (6).

The geometry parameters are: H1 (initial altitude, or sensor), H2 (final altitude or tangent height, or target), ANGLE (initial zenith angle measured from H1), RANGE (path length), BETA (earth center angle, subtended by H1 and H2), and RO (radius of the earth at point of calculation). Default RO's are given on page 35 of the LOWTRAN7 technical report. LOWTRAN7 geometry is shown in Figure 26. (All angles are in degrees and distances are in kilometers) (8).

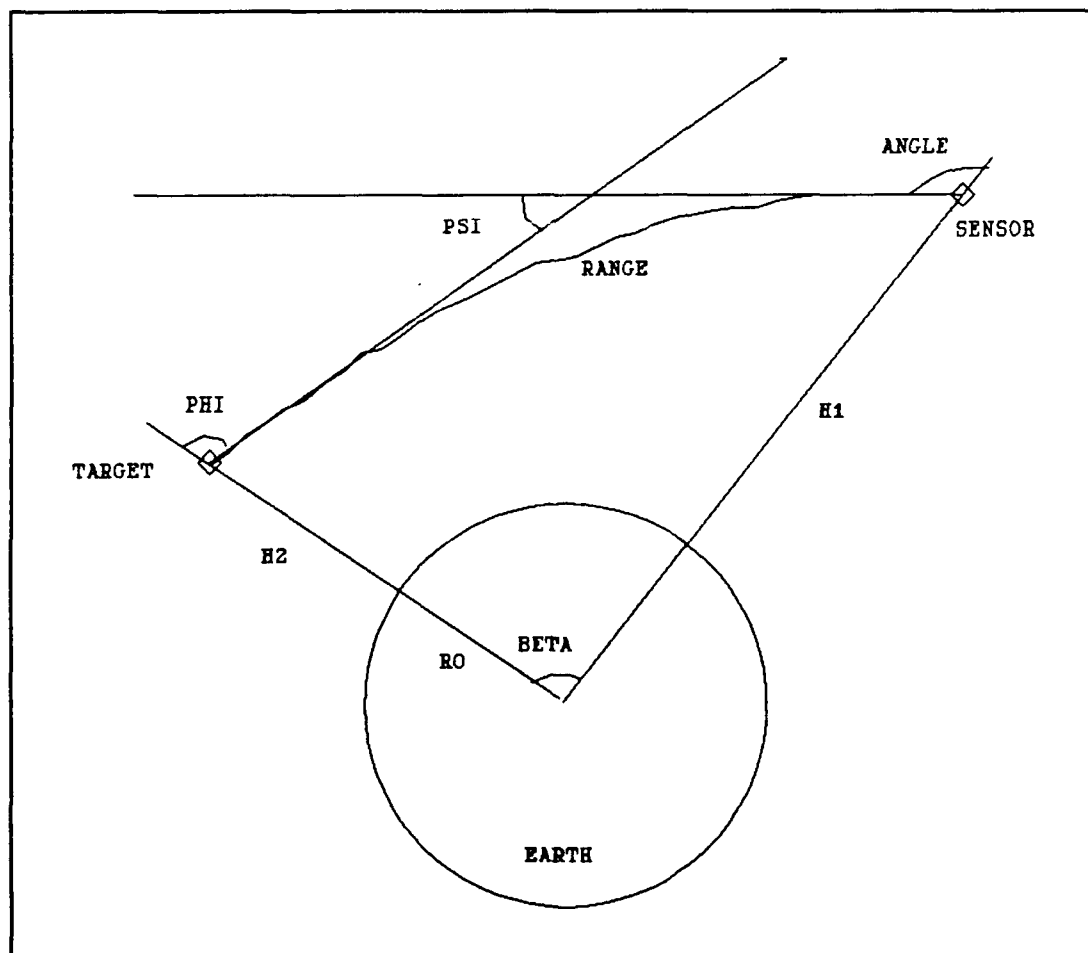


Figure 26 LOWTRAN7 GEOMETRY

For geometry 1, the inputs are:  $H1=7\text{km}$ ,  $H2=0\text{km}$ , and  $BETA=0.2^\circ$ . LOWTRAN7 calculates the rest of the geometry to be:  $ANGLE=107.55^\circ$ ,  $RANGE\approx 23\text{km}$ , and  $Bending=0.026^\circ$ . The range varies because the different atmospheric conditions cause different amounts of refraction.

In scenario 2, the inputs are:  $H1=18\text{km}$ ,  $H2=0\text{km}$ , and  $ANGLE=180^\circ$ . LOWTRAN7 calculates:  $RANGE=18\text{km}$ ,  $BETA=0^\circ$ , and no bending, as the path is vertical (8).

According to the LOWTRAN7 manual, whether or not the refractive bending of the path is considered depends on which inputs are specified, and is explained on page 36 of the LOWTRAN7 Technical Report (6). This has been changed, however, in the LOWTRAN7 version of the program. Now the refractive bending of the path is calculated for all cases, regardless of the input choices (15).

The final parameter in this card is LEN, which is only necessary (and only prompted) in certain geometrical situations. Suppose  $H1$  and  $H2$  are specified as shown:

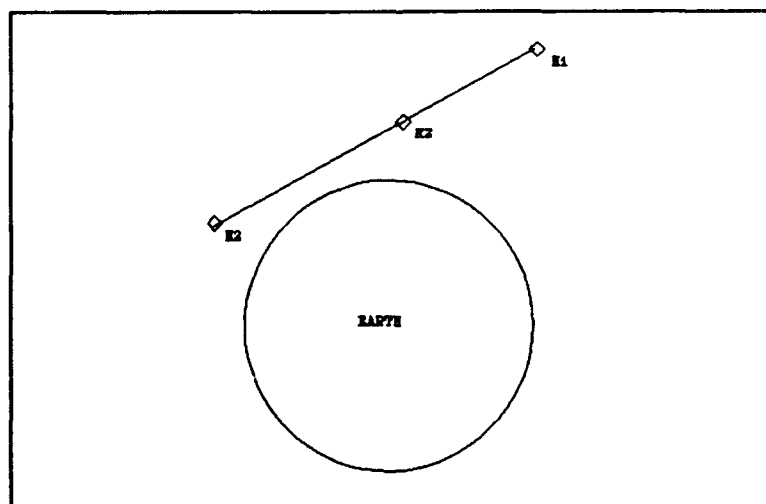


Figure 27 THE LEN OPTION  
A11

In this case, there are two possible paths the program could use to reach the given final altitude H2. The user can choose LEN = 0 for the short path or LEN = 1 for the longer path. This option can be confusing, and it seems that when in doubt, the user should choose 0 and check the geometry calculations in the output. (The LEN option will occur specifically when  $H1 > H2$  and  $ANGLE > 90^0$  are specified.) LEN is set to 0 for this study.

#### Cards 3A1 and 3A2

Since solar and lunar radiance is chosen in this study (IEMSCT = 1), there are several alternate cards that prompt the user for inputs describing the geometry of the solar/lunar source with respect to the sensor-target geometry. These inputs will be discussed in the order they are prompted by the card generator for this scenario.

#### Card 3A1

The first parameter is IPARM, and it controls how the user will specify the solar/lunar geometry (6). There are several input requirements for each choice (0, 1, or 2), but for this case the easiest to use is IPARM = 1.

The next input, IPH, determines which aerosol scattering phase function will be used, and IPH = 1 is chosen throughout this study since it requires no additional inputs. IPH=1 is the Mie scattering function, and the database for it is built into the LOWTRAN7 program.



The day of the year, IDAY, is the next input. Days 79 and 80 are used in this study, since they are around the vernal equinox. Day 79 makes the subsolar latitude  $-.46^{\circ}\text{N}$  and the subsolar longitude  $358.13^{\circ}\text{W}$ . Day 80, or March 21, makes the subsolar latitude  $-.07^{\circ}\text{N}$  and the subsolar longitude  $358.20^{\circ}\text{W}$ , so the sun is not actually directly overhead in any of these tests, but it is very close. The next choice is ISOURCE = 0 or 1, where 0 is the sun and 1 is the moon.

#### Card 3A2

The inputs of card 3A2 are determined by which value of IPARM has been selected. (If the source is the moon, IPARM=0 must be chosen.) When IPARM = 1, the inputs are the observer's latitude and longitude, the time of day (Greenwich time), and the path azimuth east of north.

To obtain maximum radiance, the target's location is  $0^{\circ}$  latitude,  $0^{\circ}$  longitude,  $0^{\circ}$  east of north, and 12.00 Greenwich time, which is at the equator on the prime meridian at 12:00 noon when the sun is almost directly overhead.

#### Card 4

Card 4 allows the user to choose what waveband the calculations will be performed in and what step sizes will be used. There are only three inputs: V1 (initial wavenumber in  $\text{cm}^{-1}$ ), V2 (final wavenumber, which must be larger than V1), and DV (frequency increment, or step size). The resolution is always  $20\text{cm}^{-1}$ ; the DV just allows the user to choose the

increments of the output wavenumbers. All three inputs are reset to the nearest 5 cm<sup>-1</sup> by the program.

All of these inputs must be in inverse centimeters (wavenumbers):

$$\bar{\nu} = \frac{1}{\lambda} \quad (27)$$

To convert from wavelength (in μm) to wavenumber (in cm<sup>-1</sup>):

$$\frac{1}{\text{wavelength}} * 10^4 = \text{wavenumber} \quad \text{Eq (28)}$$

Also

$$\Delta \nu \approx \frac{\Delta \lambda}{\lambda^2} \quad \text{Eq (29)}$$

so the average Δλ is λ<sup>2</sup>Δν, where Δν is DV.

#### Card 5

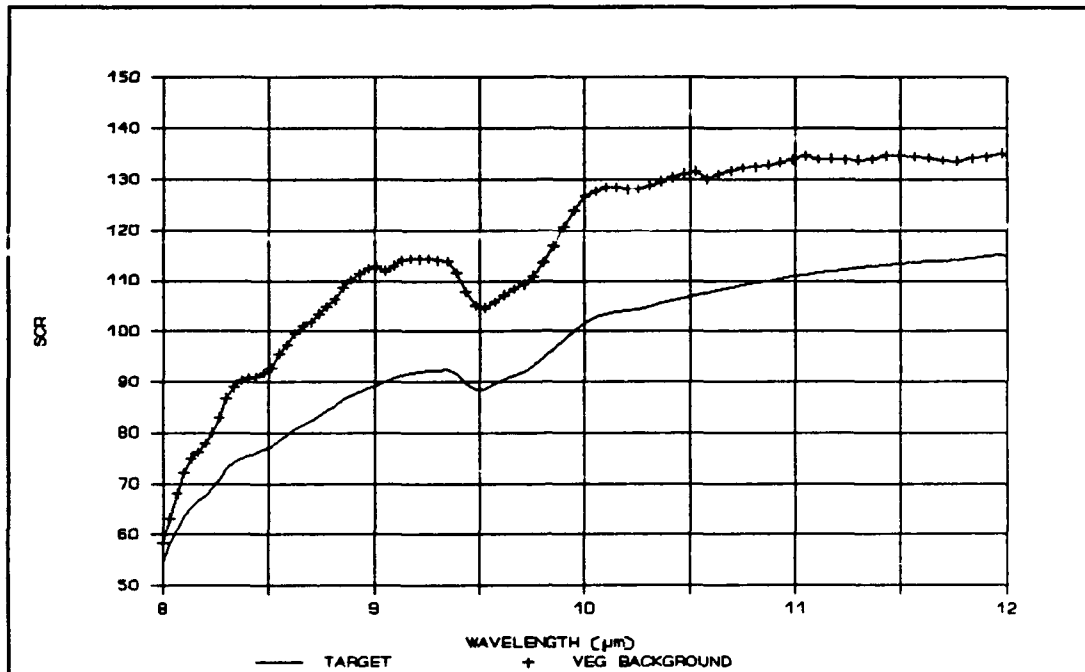
Card 5 gives the user the option of making other input selections in the same file or ending the card generation for that file (IPRT).

Once the inputs are generated, one way to alter them to make a new input file is to simply put them in an editor and edit which parameters the user wants to change. The other option is to redo the card generation. When looking at the input files (.IN7), nothing is labelled, but the inputs are in the order in which they are prompted, and each card has its own line (if the screen is wide enough). It is useful, therefore, to keep a technical report handy while editing these files.

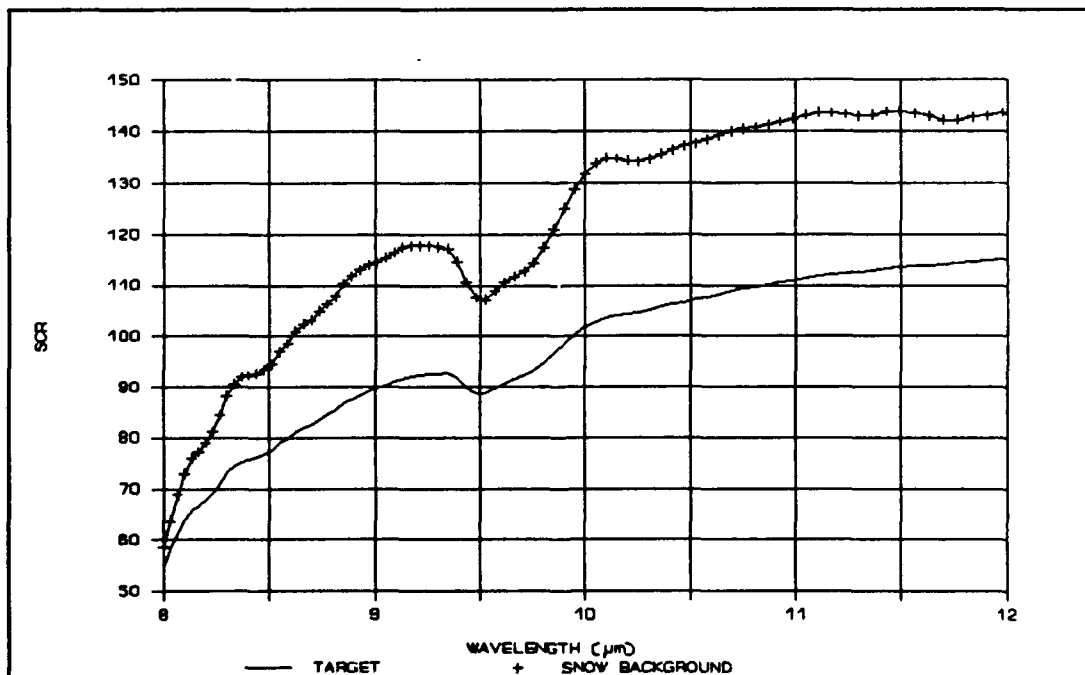
## Appendix B: Sources of Information

To really learn when and how to run and use the program, the user may need several of the following references. AFGL has published a technical report with each version of the LOWTRAN model. Each technical report assumes that the user knows what is in all of the preceding technical reports, so the user may have to refer to more than one of them to get desired information. Many of the equations that are changed in the program do not get changed in the technical reports, and the user should be aware of this fact. There are also several other technical reports, many of which are mentioned in the references of this study, that the user may find helpful. For example, the technical report, AFGL Atmospheric Constituent Profiles (12), contains the atmospheric profiles for the various model choices used in LOWTRAN7, along with other possibly useful information. Another helpful source is the Handbook of Geophysics and the Space Environment (13). A very good source of information is the individuals who wrote it, and the people who have used it a lot (such as Air Force Staff Meteorologists, etc.).

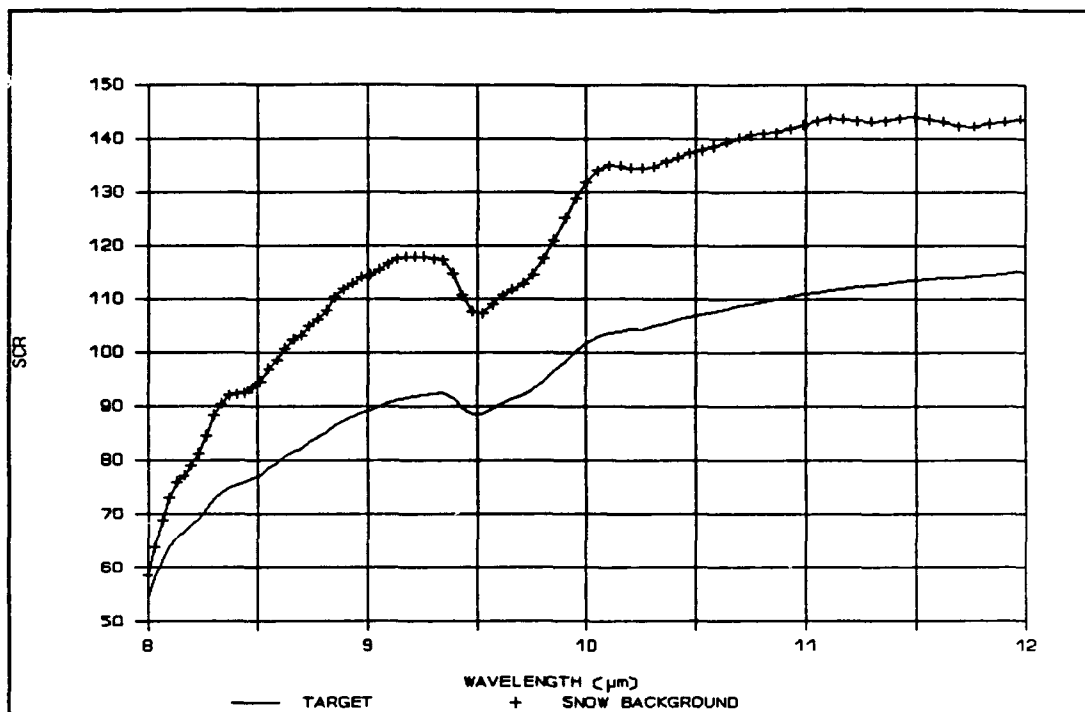
## Appendix C: Figures and Tables of Data



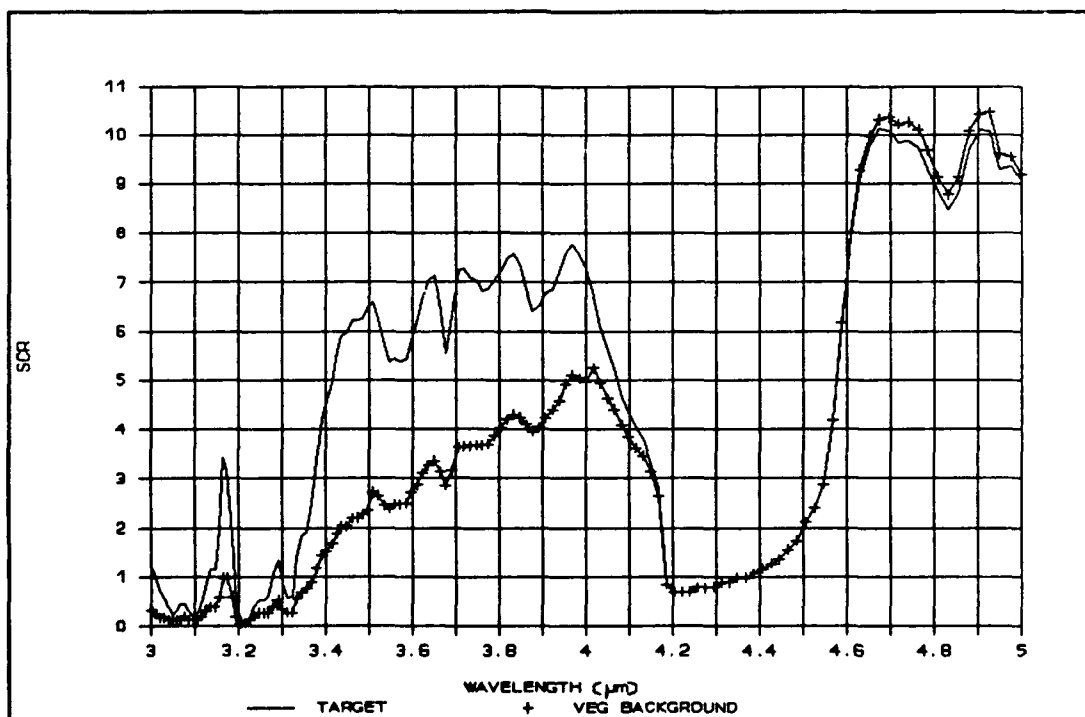
**Figure 1** SCRs FOR NIGHTTIME, SCENARIO 1, VEGETATION BACKGROUND, HgCdTe DETECTOR



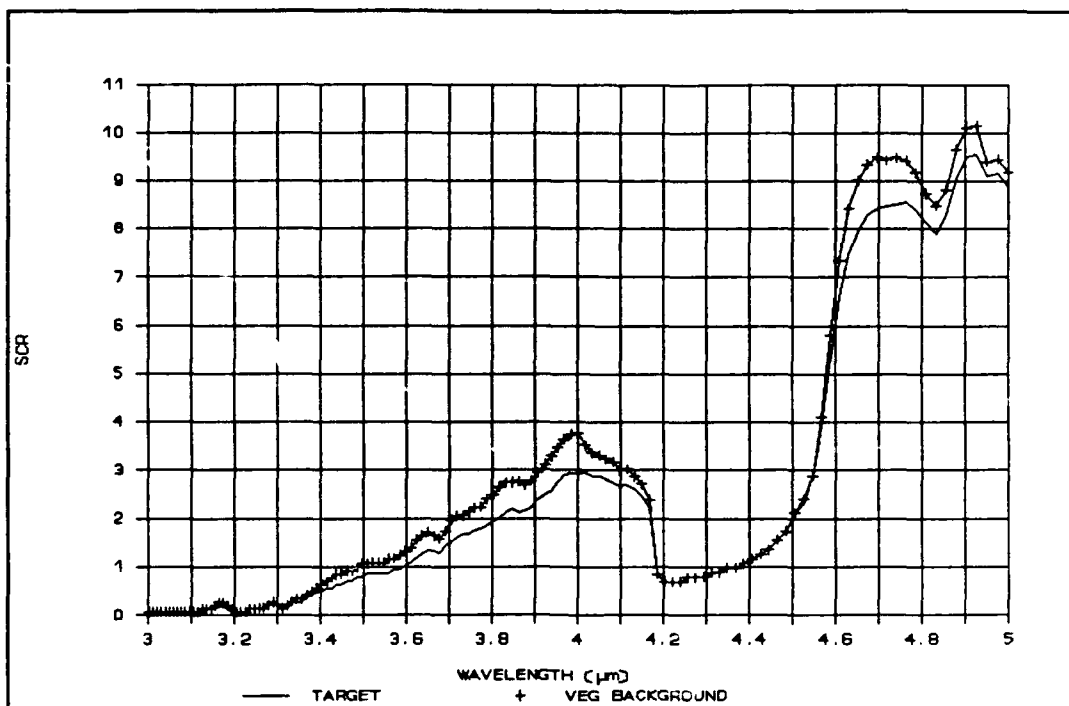
**Figure 2** SCRs FOR DAYTIME, SCENARIO 1, SNOW BACKGROUND, HgCdTe DETECTOR



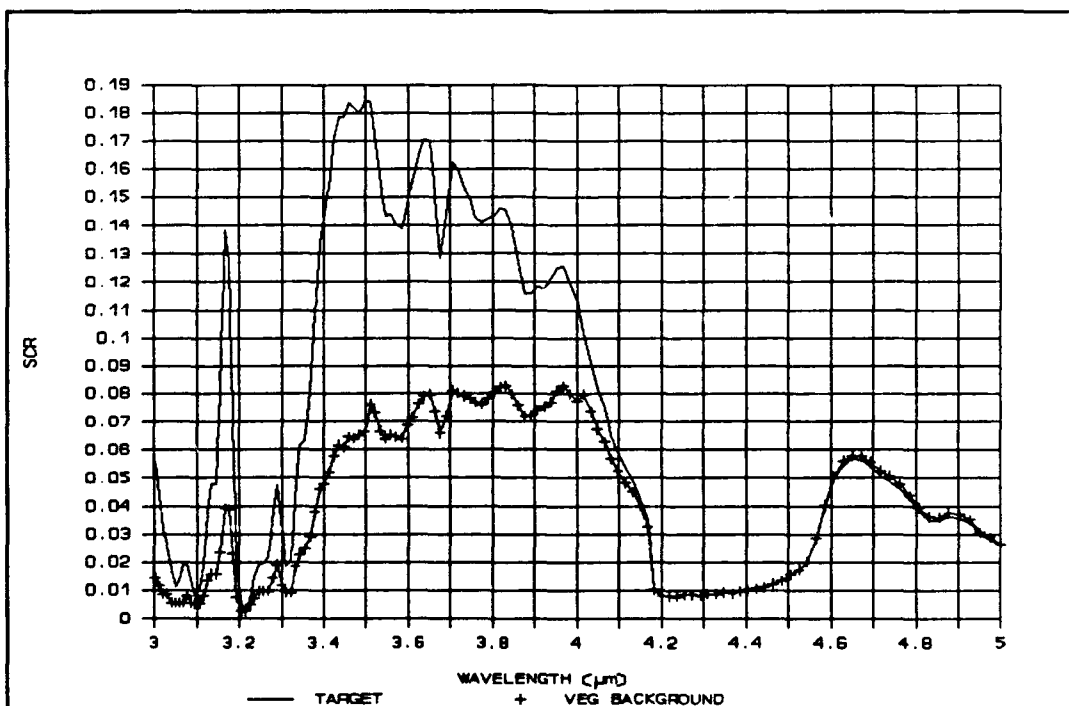
**Figure 3** SCRs FOR NIGHTTIME, SCENARIO 1, SNOW BACKGROUND HgCdTe DETECTOR



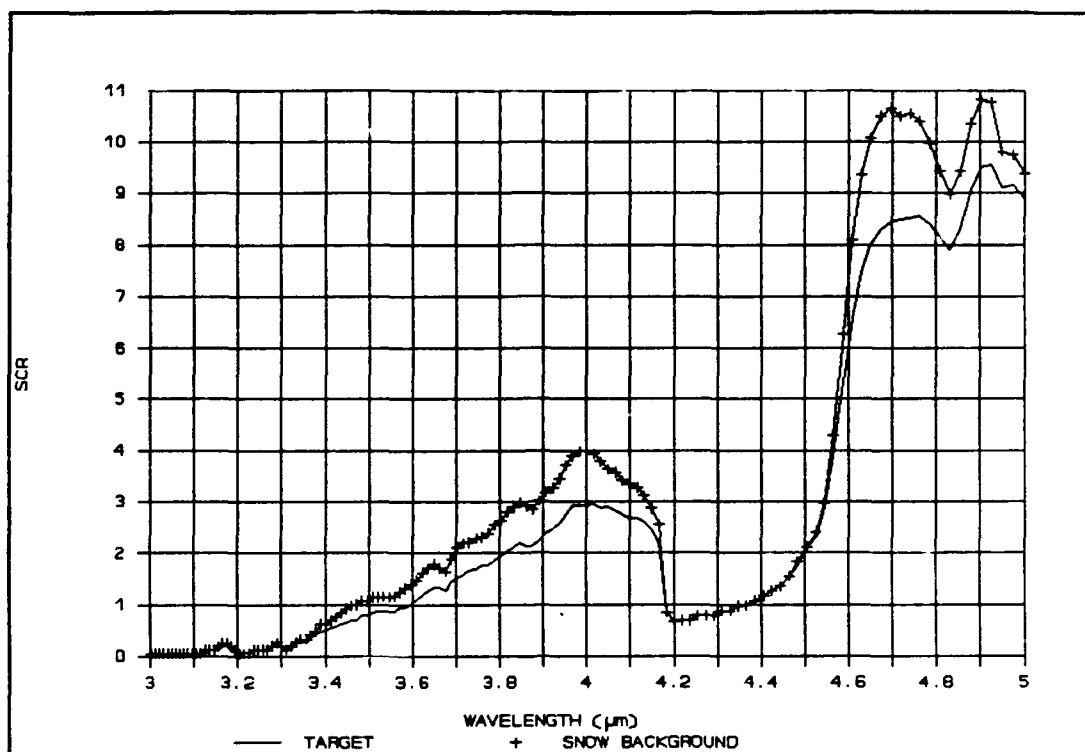
**Figure 4** SCRs FOR DAYTIME, SCENARIO 1, VEGETATION BACKGROUND, InSb DETECTOR



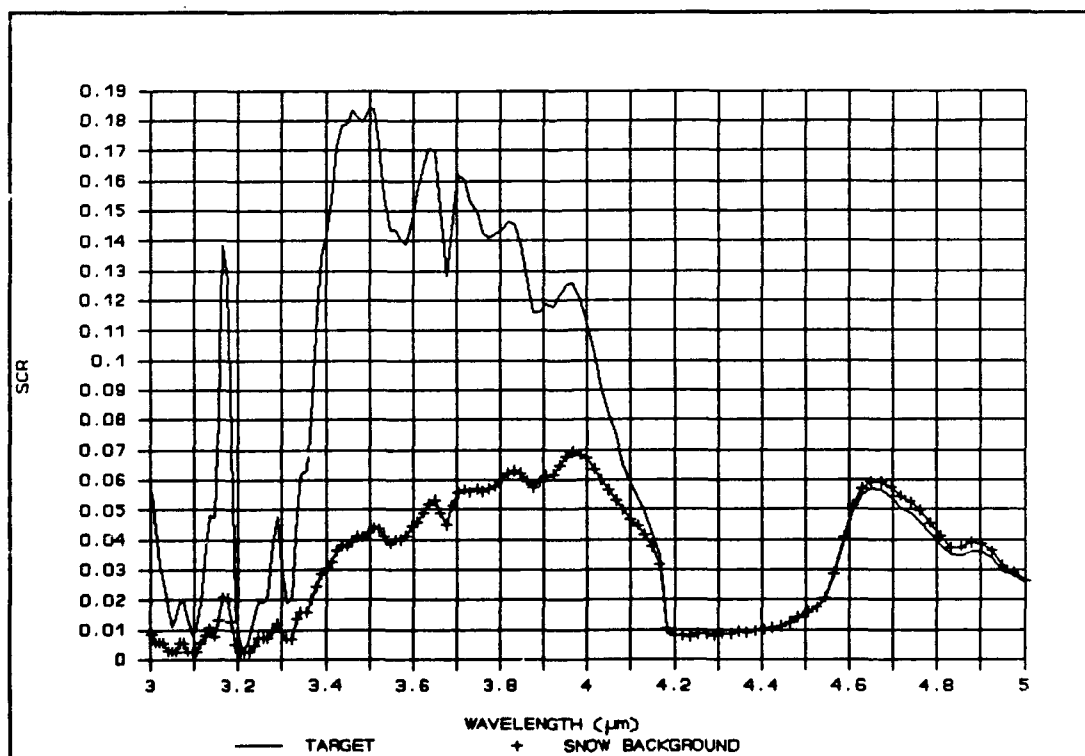
**Figure 5** SCRs FOR NIGHTTIME, SCENARIO 1, VEGETATION BACKGROUND, InSb DETECTOR



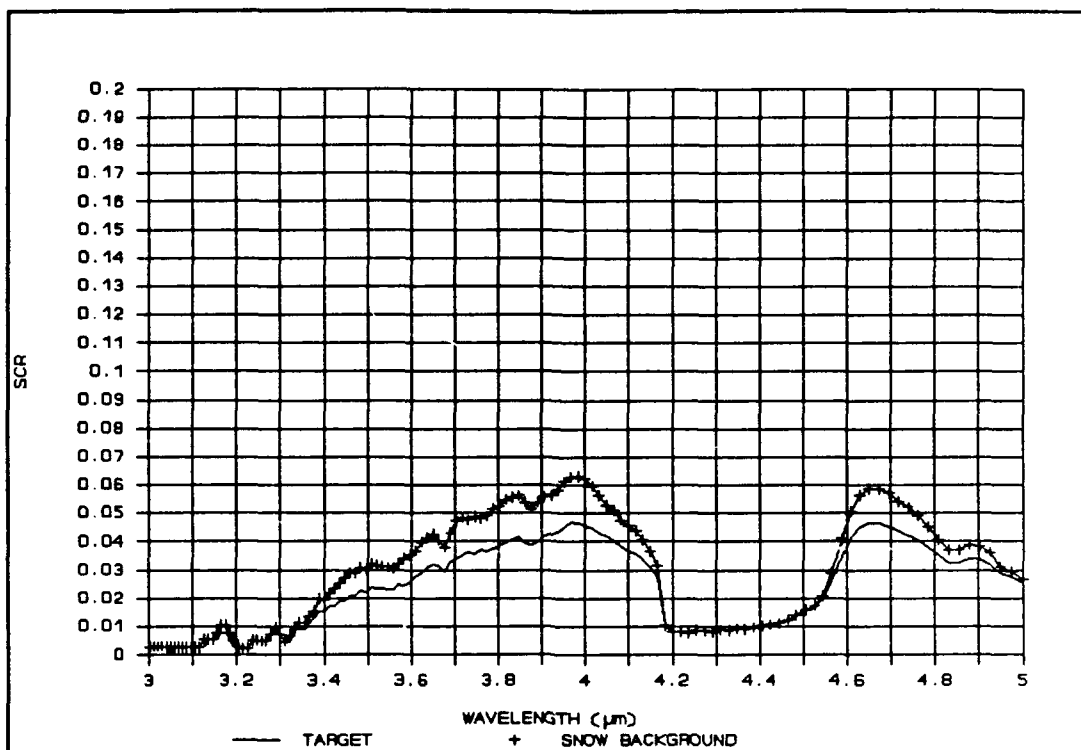
**Figure 6** SCRs FOR DAYTIME, SCENARIO 1, VEGETATION BACKGROUND, PtSi DETECTOR



**Figure 9** SCRs FOR NIGHTTIME, SCENARIO 1, SNOW BACKGROUND, InSb DETECTOR



**Figure 10** SCRs FOR DAYTIME, SCENARIO 1, SNOW BACKGROUND, PtSi DETECTOR



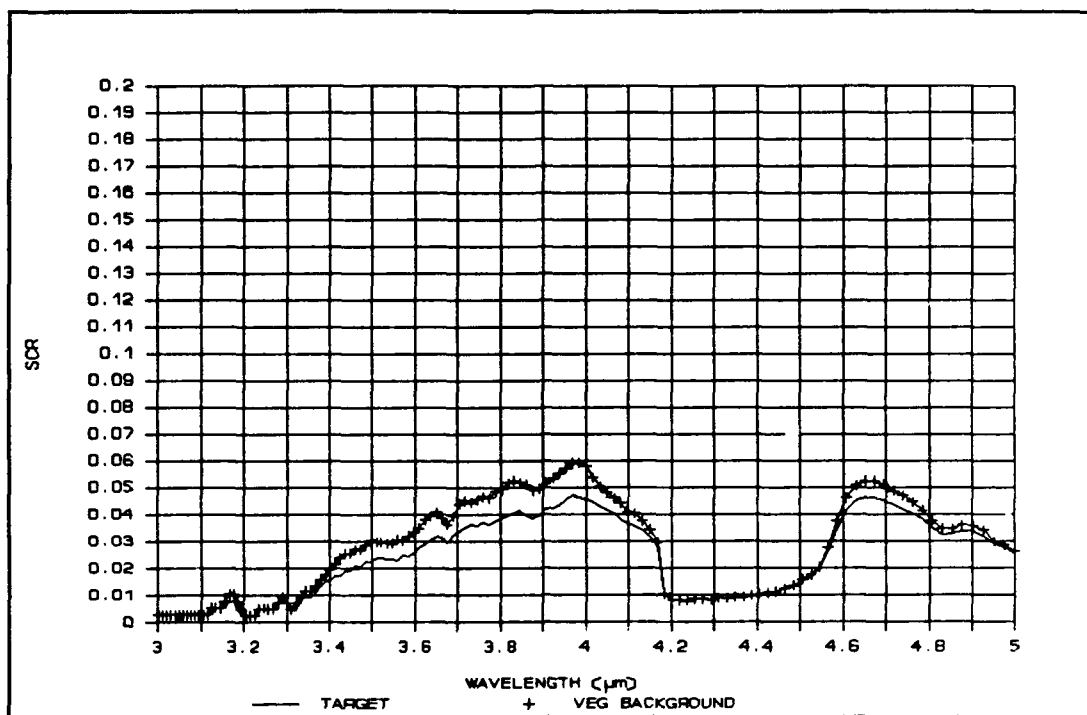
**Figure 11** SCRs FOR NIGHTTIME, SCENARIO 1, SNOW BACKGROUND, PtSi DETECTOR

Table C1

Average Contrasts (%) Calculated  
When Varying Relative Humidity  
in Scenario 1, 3.3-4.2 and 8-12 Bands

Relative Humidity Increase from Standard Atmosphere	InSb Day (3.3-4.2)	InSb Night (3.3-4.2)	PtSi Day (3.3-4.2)	PtSi Night (3.3-4.2)	HgCdTe Day (8-12)	HgCdTe Night (8-12)
10%	46.84	22.81	50.70	23.69	19.06	19.24
20%	46.09	22.80	49.99	23.89	16.99	17.16
30%	45.27	22.04	49.10	22.93	14.99	15.14
40%	44.44	21.63	48.31	22.65	13.04	13.16
48%	43.57	21.07	47.42	21.97	11.51	11.62





**Figure 7** SCRs FOR NIGHTTIME, SCENARIO 1, VEGETATION BACKGROUND, Ptsi DETECTOR

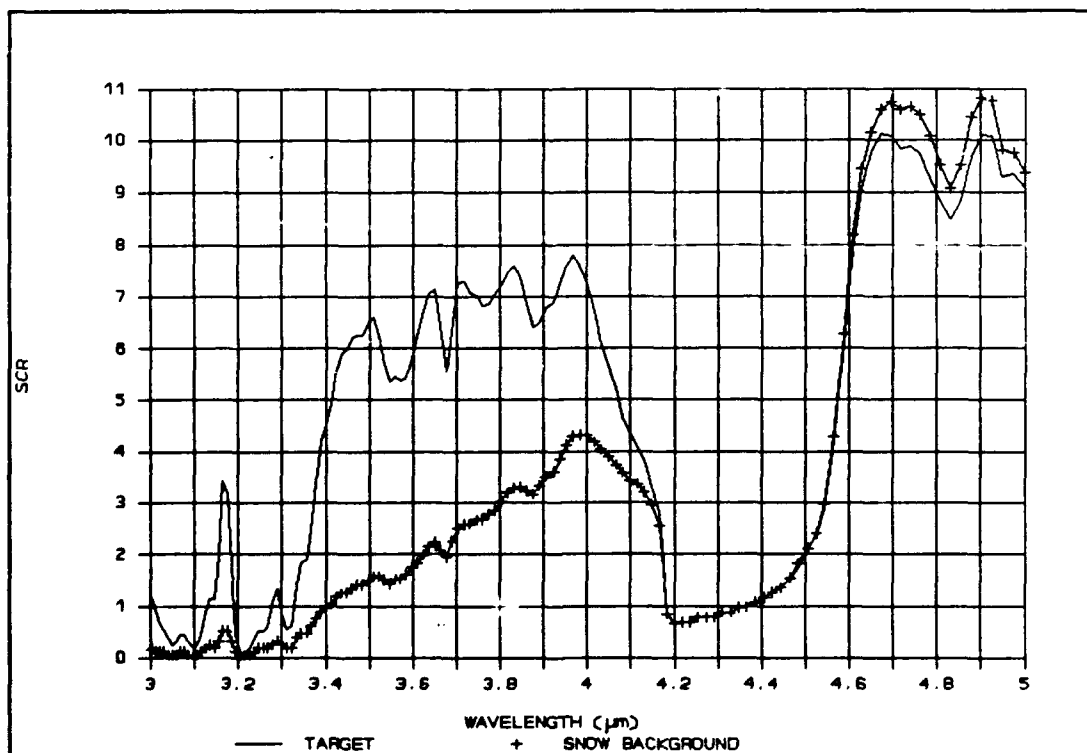


**Figure 8** SCRs FOR DAYTIME, SCENARIO 1, SNOW BACKGROUND, InSb DETECTOR

Table C2

Average Contrasts (%) Calculated  
When Varying Absolute Humidity in Scenario 1

Absolute Humidity Increase from Standard Atmosphere	InSb Day (3.3-4.2)	InSb Night (3.3-4.2)	PtSi Day (3.3-4.2)	PtSi Night (3.3-4.2)	HgCdTe Day (8-12)	HgCdTe Night (8-12)
10%	47.75	23.65	51.61	24.69	21.52	21.74
20%	47.48	24.04	51.36	25.19	20.66	20.86
30%	47.14	23.62	50.98	24.74	19.78	19.97
40%	46.95	23.40	50.79	24.49	18.92	19.10
50%	46.51	22.76	50.34	23.62	18.03	18.19

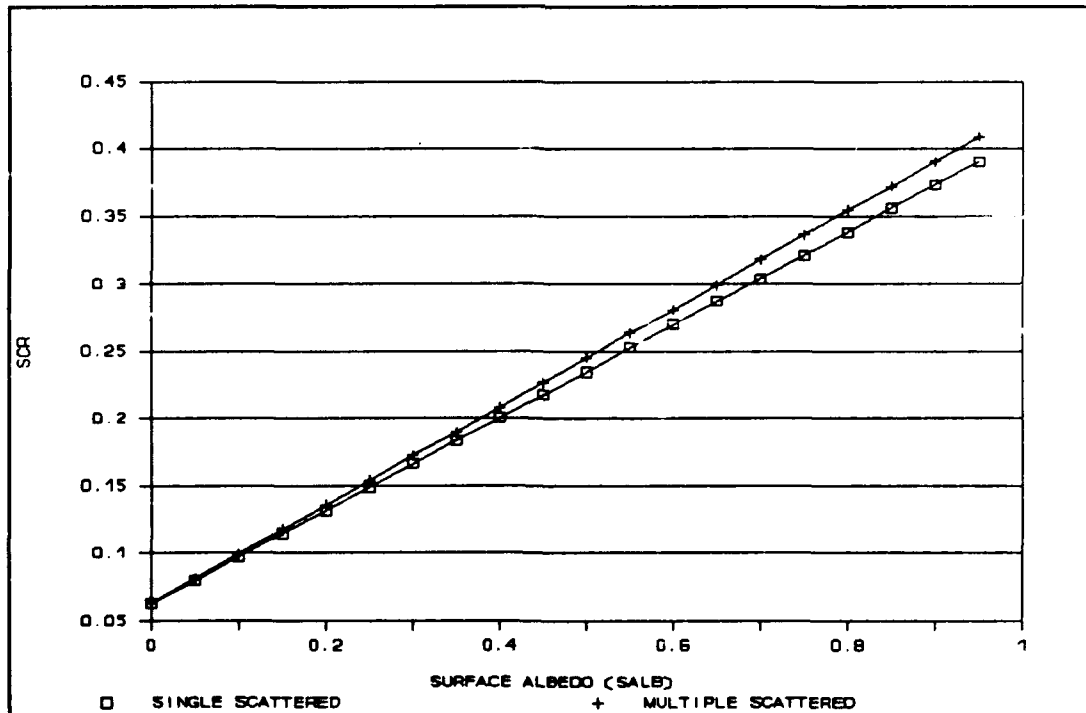


**Figure 12 SCR EVALUATED AT 3.802 $\mu$ m, PtSi DETECTOR, DAY**

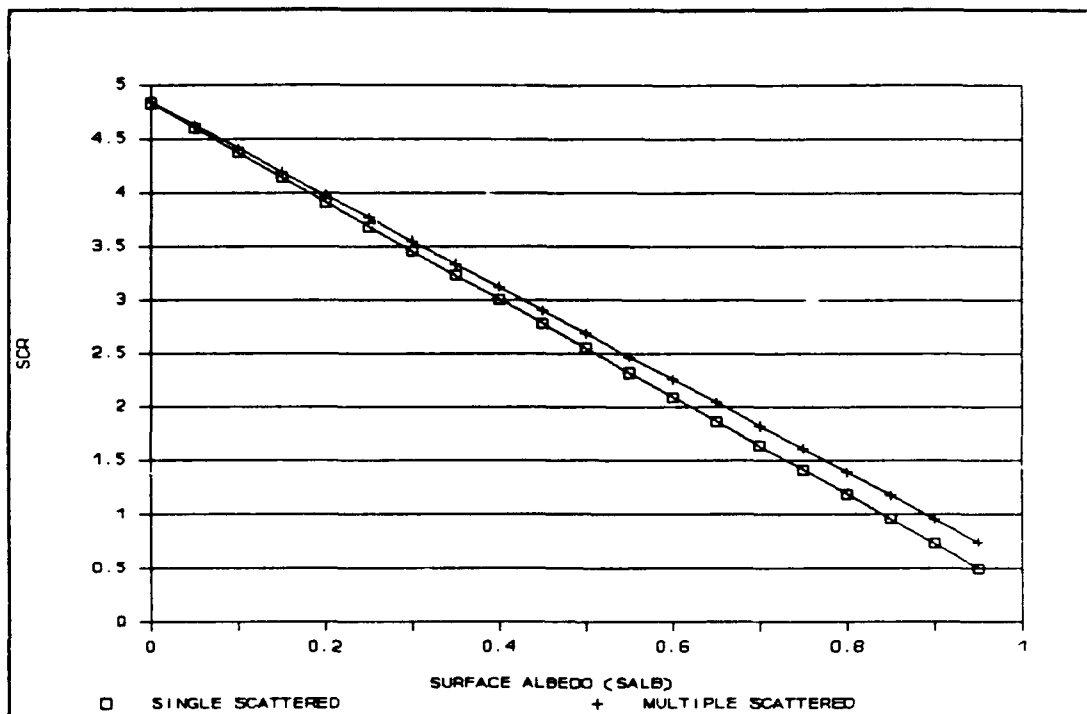


Figure 13 SCR EVALUATED AT 4.00 $\mu$ m, InSb DETECTOR, NIGHT

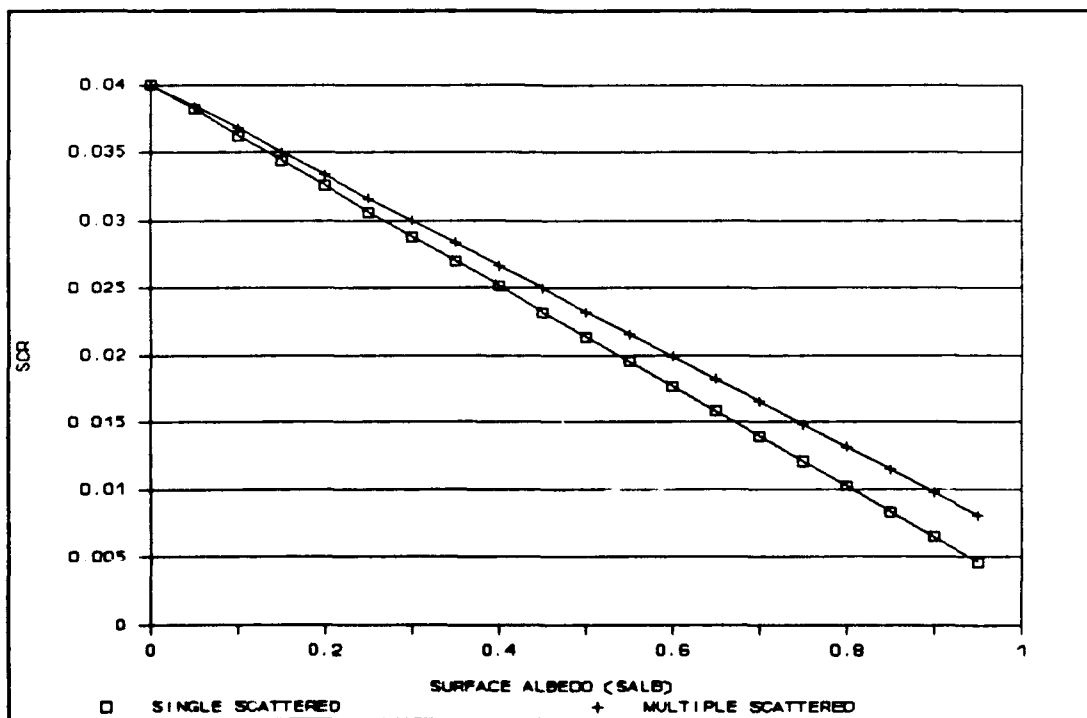


Figure 14 SCR EVALUATED AT 3.509 $\mu$ m, PtSi DETECTOR, NIGHT

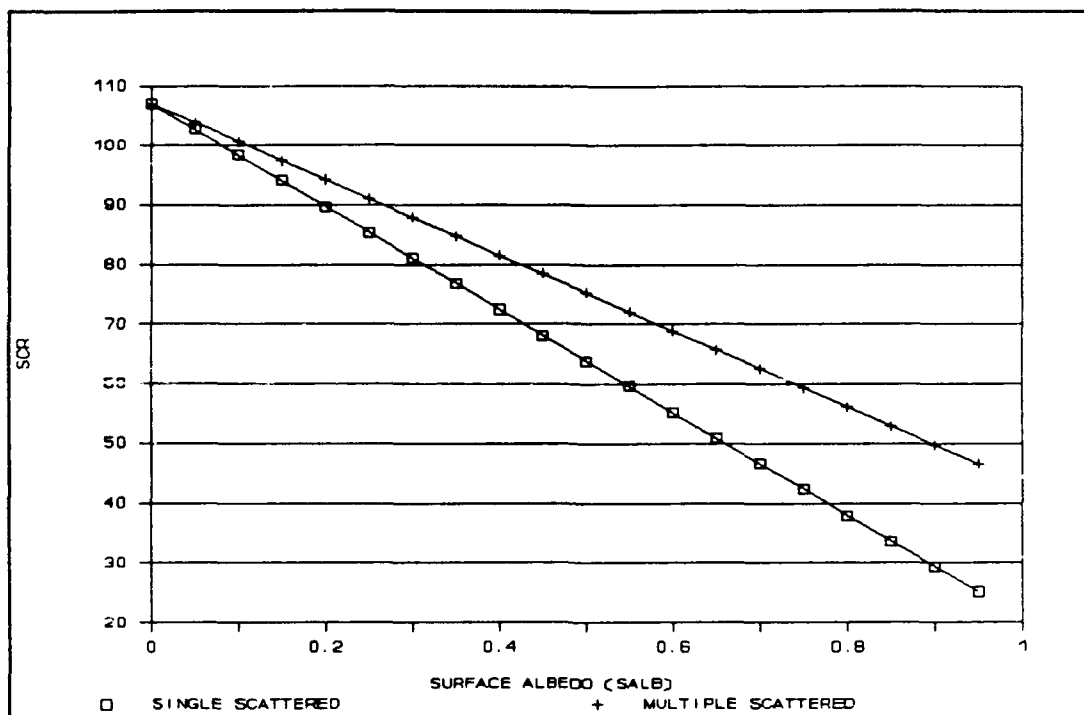


Figure 15 SCR EVALUATED AT 8.511 $\mu$ m, HgCdTe DETECTOR, DAY

## Appendix D: Terms and Definitions

The following is a list of terms used throughout this paper.

Background - The material surrounding the target. A mixture of vegetations and snow are the two backgrounds used in this study. They are assumed to be homogeneous across the footprint of the sensor.

Boundary - Anything that is at the end of the path. This could be a target, boundary, cloud, atmospheric layer, etc., or a mixture of any of the above.

Change in Signal (CS) - A figure-of-merit used in this study to evaluate the non-imaging system. The difference between the output signal when the target is in the field-of-view divided by the signal when the target is not in the field-of-view.

Contrast - A figure-of-merit used to evaluate the imaging system in this paper. The difference between output signal due to the target and the output signal due to the background divided by the output signal due to the target.

Detection System (Sensor) - Composed of an equivalent lens and a detector or an array of detectors. The lens focuses radiation onto the detector(s), and electrons are photoexcited to produce current.

Field-of-View - The volume of space the detector "sees".

Footprint - The area on the ground or at the end of the path that the detector "sees".

Imaging System - Utilizes a lens and more than one detector. In this paper it is assumed that the target is large compared to the field-of-view of one detector (or the instantaneous field-of-view).

Non-Imaging System - Utilizes a lens and a single detector. In this paper it is assumed that the target is small compared to the field-of-view of the detector.

Path - The stretch of space between a sensor and the boundary.

Radiance - In this paper 'radiance' refers to the amount of radiance that reaches the sensor from some source after travelling across some path, or the transmitted radiance. All LOWTRAN7 'radiance' outputs are actually transmitted radiances.

SCR (Scaled Count Rate) - Count of the photoexcited electrons in the detector when radiation is incident upon it.

Sensor - Composed of an equivalent lens and a detector or an array of detectors. The lens focuses radiation onto the detector(s), and electrons are photoexcited to produce current.

Target - The object that the sensor is trying to detect or discriminate.

Transmittance - The fraction of radiation from one point in space that reaches another point in space.

## Bibliography

1. Cantella, Michael J. Space Surveillance Application Potential of Schottky Barrier IR Sensors. Contract F192885C002. Lexington, Massachusetts: Lincoln Laboratory, Massachusetts Institute of Technology, 9 April 1987 (AD-A180848).
2. Lange, J. J., and R. R. Sandys. Phenomenology/Sensitivity Analysis of Platinum Silicide, Indium Antimonide, and Mercury-Cadmium-Telluride Detector Performance in the 3 to 5 Micrometer Infrared Bank for Air-to-Ground Applications. Presented at the 1990 IRIS Specialty Group on Passive Sensors, 14 March, 1990, Applied Physics Lab, Johns Hopkins University, Laurel Md.
3. McCartney, Earl J. Optics of the Atmosphere. New York: John Wiley and Sons, 1976.
4. Kneizys, F. X. et al. Atmospheric Transmittance/Radiance: Computer Code LOWTRAN6. AFGL Technical Report 83-0187. Optical Physics Division, Air Force Geophysics Laboratory, Hanscomb AFB MA, 1 August, 1983.
5. Selby, J. E. A., and R. M. McClatchey. Atmospheric Transmittance from 0.25 to 28.5 Micrometers: Computer Code LOWTRAN2. AFCRL-72-0745. Optical Physics Laboratory, Air Force Cambridge Research Laboratories, Hanscomb Field MA, 29 December 1972 (AD-763721).
6. Kneizys, F. X. et al. Users Guide to LOWTRAN 7. AFGL Technical Report 88-0177. Optical/Infrared Technology Division, Air Force Geophysics Lab, Hanscomb AFB MA, 16 August, 1988 (AD-A206773).
7. Kneizys, F. X. Personal interviews. Air Force Geophysics Lab, Hanscomb AFB MA, Summer 1990.
8. Kneizys, F. X. et al. Atmospheric Transmittance/Radiance: Computer Code LOWTRAN5. AFGL Technical Report 80-0067. Optical Physics Division, Air Force Geophysics Laboratory, Hanscomb AFB MA 21 February, 1980 (AD-A088215).
9. Turner, R. E., "Thermophysical Properties of Natural Surface Materials," Science Applications International Corporation, Dayton OH, Oct 85, AFWAL-TR-88-1068, AD - B102596.

10. Berger, R. H., "Snowpack Optical Properties in the Infrared," US Army Cold Regions Research and Engineering Laboratory, Hanover NH, May 79, CRREL-79-11, AD - A071004.
11. Hudson, Richard D., Jr. Infrared System Engineering. New York: John Wiley & Sons, 1969.
12. Anderson, G. P. et al. AFGL Atmospheric Profiles (0-120km). AFGL Technical Report 86-0110. Optical Physics Division, Air Force Geophysics Laboratory, Hanscomb AFB MA, 15 May, 1986.
13. Aarons, J. et al. Handbook of Geophysics and the Space Environment, Springfield, VA: National Technical Information Center, 1985.
14. Roadcap, Major. Personal interviews. Air Force Staff Meteorology, Wright-Patterson AFB OH, Summer 1990.
15. Weaver, Sandra. Personal interviews. Air Force Staff Meteorologist, Wright-Patterson AFB, OH, Summer 1990.
16. Condray, Patrick M., "A LOWTRAN7 Sensitivity Study in the 8-12 and 3-5 Micron Bands," USAF Environmental Technical Applications Center, Scott AFB IL, Feb 1990, USAFETAC-TN-90-002.
17. Smith, Elske v. P. and Michael Zeilik. Introductory Astronomy and Astrophysics. Philadelphia: Saunders College Publishing, 1987.



### Vita

Second Lieutenant Kelli J. Owen was born on 20 July 1967 in Nashville, Tennessee. She graduated from McGavock High School in Nashville, Tennessee, in 1985. She then attended the United States Air Force Academy, graduating with a Bachelor of Science in Space Physics in 1989. Upon graduation, she entered the School of Engineering, Air Force Institute of Technology, in July, 1989.

Permanent Address: 2334 Ridgeland Drive

Nashville, Tennessee 37214

# REPORT DOCUMENTATION PAGE

Form Approved  
OMB No. 0704-0188

Public reporting burden for this collection of information is estimated to average 1 hour per response, including the time for reviewing instructions, searching existing data sources, gathering and maintaining the data needed, and completing and reviewing the collection of information. Send comments regarding this burden estimate or any other aspect of this collection of information, including suggestions for reducing this burden, to Washington Headquarters Services, Directorate for Information Operations and Reports, 1215 Jefferson Davis Highway, Suite 1204, Arlington, VA 22202-4302, and to the Office of Management and Budget, Paperwork Reduction Project (0704-0188), Washington, DC 20503.

1. AGENCY USE ONLY (Leave blank)		2. REPORT DATE December 1990	3. REPORT TYPE AND DATES COVERED Master's Thesis	
4. TITLE AND SUBTITLE THE USE OF THE LOWTRAN7 ATMOSPHERIC TRANSMITTANCE AND RADIANCE MODEL FOR DETECTION SYSTEM DESIGN AND ANALYSIS			5. FUNDING NUMBERS	
6. AUTHOR(S) Kelli J. Owen, 2nd Lieutenant, USAF				
7. PERFORMING ORGANIZATION NAME(S) AND ADDRESS(ES) Air Force Institute of Technology, WPAFB OH 45433-6583			8. PERFORMING ORGANIZATION REPORT NUMBER AFIT/GEP/ENP/90D-3	
9. SPONSORING / MONITORING AGENCY NAME(S) AND ADDRESS(ES)			10. SPONSORING / MONITORING AGENCY REPORT NUMBER	
11. SUPPLEMENTARY NOTES				
12a. DISTRIBUTION AVAILABILITY STATEMENT Approved for public release; distribution unlimited			12b. DISTRIBUTION CODE	
13. ABSTRACT (Maximum 200 words) The purpose of this study is to demonstrate how the LOWTRAN7 computer model can be used for detection system design and analysis. The LOWTRAN7 code is an atmospheric model that performs low resolution (20cm-1 bandwidth) calculations to estimate atmospheric transmittance and radiance under a given set of conditions. Generic imaging and non-imaging systems are analyzed. A hypothetical figure-of-merit is evaluated for each type of system using the transmittance and radiance calculated by LOWTRAN7. The figure-of-merit calculated for the imaging system is contrast, the difference between the target and background input signals divided by the target input signal. The figure-of-merit evaluated for the non-imaging system is the change in signal (CS), the difference between the input signal with the target in the field-of-view and the input signal without the target in the field-of-view divided by the input signal without the target in the field-of-view. Changing atmospheric, target, and background characteristics in LOWTRAN7 has different effects on the figures-of-merit. The characteristics tested are: background emissivity, target temperature, boundary layer aerosols, atmospheric profiles, relative humidity, and absolute humidity. Two different sensor-target geometries using different paths are studied.				
14. SUBJECT TERMS LOWTRAN, Atmospheric Modeling, Atmospheric Physics, Atmospheric Transmittance, Infrared Transmittance, MODTRAN			15. NUMBER OF PAGES 112	
			16. PRICE CODE	
17. SECURITY CLASSIFICATION OF REPORT Unclassified	18. SECURITY CLASSIFICATION OF THIS PAGE Unclassified	19. SECURITY CLASSIFICATION OF ABSTRACT Unclassified	20. LIMITATION OF ABSTRACT UL	

## GENERAL INSTRUCTIONS FOR COMPLETING SF 298

The Report Documentation Page (RDP) is used in announcing and cataloging reports. It is important that this information be consistent with the rest of the report, particularly the cover and title page. Instructions for filling in each block of the form follow. It is important to **stay within the lines** to meet optical scanning requirements.

**Block 1. Agency Use Only (Leave blank).**

**Block 2. Report Date.** Full publication date including day, month, and year, if available (e.g. 1 Jan 88). Must cite at least the year.

**Block 3. Type of Report and Dates Covered.** State whether report is interim, final, etc. If applicable, enter inclusive report dates (e.g. 10 Jun 87 - 30 Jun 88).

**Block 4. Title and Subtitle.** A title is taken from the part of the report that provides the most meaningful and complete information. When a report is prepared in more than one volume, repeat the primary title, add volume number, and include subtitle for the specific volume. On classified documents enter the title classification in parentheses.

**Block 5. Funding Numbers.** To include contract and grant numbers; may include program element number(s), project number(s), task number(s), and work unit number(s). Use the following labels:

C - Contract	PR - Project
G - Grant	TA - Task
PE - Program Element	WU - Work Unit Accession No.

**Block 6. Author(s).** Name(s) of person(s) responsible for writing the report, performing the research, or credited with the content of the report. If editor or compiler, this should follow the name(s).

**Block 7. Performing Organization Name(s) and Address(es).** Self-explanatory

**Block 8. Performing Organization Report Number.** Enter the unique alphanumeric report number(s) assigned by the organization performing the report.

**Block 9. Sponsoring/Monitoring Agency Name(s) and Address(es).** Self-explanatory.

**Block 10. Sponsoring/Monitoring Agency Report Number.** (If known)

**Block 11. Supplementary Notes.** Enter information not included elsewhere such as: Prepared in cooperation with...; Trans. of...; To be published in.... When a report is revised, include a statement whether the new report supersedes or supplements the older report.

**Block 12a. Distribution/Availability Statement.** Denotes public availability or limitations. Cite any availability to the public. Enter additional limitations or special markings in all capitals (e.g. NOFORN, REL, ITAR).

**DOD** - See DoDD 5230.24, "Distribution Statements on Technical Documents."

**DOE** - See authorities.

**NASA** - See Handbook NHB 2200.2.

**NTIS** - Leave blank.

**Block 12b. Distribution Code.**

**DOD** - Leave blank.

**DOE** - Enter DOE distribution categories from the Standard Distribution for Unclassified Scientific and Technical Reports.

**NASA** - Leave blank.

**NTIS** - Leave blank.

**Block 13. Abstract.** Include a brief (*Maximum 200 words*) factual summary of the most significant information contained in the report.

**Block 14. Subject Terms.** Keywords or phrases identifying major subjects in the report.

**Block 15. Number of Pages.** Enter the total number of pages.

**Block 16. Price Code.** Enter appropriate price code (*NTIS only*).

**Blocks 17. - 19. Security Classifications.** Self-explanatory. Enter U.S. Security Classification in accordance with U.S. Security Regulations (i.e., UNCLASSIFIED). If form contains classified information, stamp classification on the top and bottom of the page.

**Block 20. Limitation of Abstract.** This block must be completed to assign a limitation to the abstract. Enter either UL (unlimited) or SAR (same as report). An entry in this block is necessary if the abstract is to be limited. If blank, the abstract is assumed to be unlimited.